Mycobacterium tuberculosis PPE60 antigen drives Th1/Th17 responses via Toll-like receptor 2–dependent maturation of dendritic cells

Received for publication, January 4, 2018, and in revised form, April 11, 2018 Published, Papers in Press, May 8, 2018, DOI 10.1074/jbc.RA118.001696

Haibo Su[‡§1], **Zhen Zhang**[§1], **Zijian Liu**[‡], **Baozhou Peng**[‡], **Cong Kong**[¶], **Honghai Wang**[¶], **Zhi Zhang**[§2], and **Ying Xu**[¶3]

From the [‡]*GMU-Guangzhou Institutes of Biomedicine and Health (GIBH) Joint School of Life Science, Guangzhou Medical University (GMU), Number 195 Dongfengxi Road, Guangzhou 510000, China,* [¶]*State Key Laboratory of Genetic Engineering, Institute of Genetics, School of Life Science, Fudan University, Number 220 Handan Road, Shanghai 200433, China, and* [§]*Guangdong Second Provincial General Hospital, Number 466 Xingang Road, Guangzhou 510220, China*

Edited by Charles E. Samuel

Targeting of *Mycobacterium tuberculosis* (MTB) PE/PPE antigens that induce type 1 helper T cell (Th1) and Th17 responses represents a crucial strategy for the development of tuberculosis (TB) vaccines. However, only a few PE/PPE antigens induce these responses. Here, we sought to determine how the cell wall–associated antigen PPE60 (Rv3478) activates dendritic cell (DC) maturation and T-cell differentiation. We observed that PPE60 induces DC maturation by augmenting the protein expression of cluster of differentiation 80 (CD80) and CD86 and major histocompatibility complex (MHC) class I and MHC class II on the cell surface. PPE60 also stimulated the production of tumor necrosis factor-α (TNFα), interleukin (IL)-1β, IL-6, IL-12p70, and IL-23p19 but not IL-10. This induction was mediated by Toll-like receptor 2 (TLR2) and followed by activation of p38, c-Jun N-terminal kinase (JNK), and NF-κB signaling. PPE60 enhanced MHC-II expression and promoted antigen processing by DCs in a TLR2-dependent manner. Moreover, PPE60-stimulated DCs directed naïve CD4$^+$ T cells to produce IFN-γ, IL-2, and IL-17A, expanding the Th1 and Th17 responses, along with activation of T-bet and RAR-related orphan receptor C (RORγt) but not GATA-3. Moreover, PPE60 activated the NLRP3 inflammasome followed by caspase-1–dependent IL-1β and IL-18 synthesis in DCs. Of note, pharmacological inhibition of NLRP3 activation specifically attenuated IFN-γ and IL-17A secretion into the supernatant from CD4$^+$ T cells cocultured with PPE60-activated DCs. These findings indicate that PPE60 induces Th1 and Th17 immune responses by activating DCs in a TLR2-dependent manner, suggesting PPE60's potential for use in MTB vaccine development.

Mycobacterium tuberculosis (MTB),[4] the causative agent of human tuberculosis, has shown an outstanding ability to adapt to its host (1). Indeed, greater than one-third of the world's population is latently infected with this organism, and millions of people succumb to MTB infection each year (2). Due to the current epidemic fueled by human immunodeficiency virus (HIV) coinfection and increasing spread of drug-resistant MTB strains, the resurgence of pulmonary tuberculosis is an ongoing threat to global health (3). Currently, the only available *Mycobacterium bovis* bacillus Calmette-Guérin (BCG) vaccine is of limited efficacy against pulmonary tuberculosis in young adults, in reactivated populations, and in TB-endemic regions (4, 5). The ineffectiveness of BCG, the noncompliance of TB drugs, and the emergence of individuals coinfected with HIV and MTB highlight the importance of the development of a new and improved vaccine.

The PE/PPE family proteins from MTB are named after the presence of their conserved N-terminal Pro-Glu (PE) or Pro-Pro-Glu (PPE) motifs (6). 99 *pe* and 69 *ppe* genes represent ~10% of the genome and are characterized by their high GC content and extensive repetitive homologous sequences (7). Although the detailed function of this gene family remains to be unraveled, PE/PPE genes are strongly suspected to be associated with several aspects of host–pathogen interactions, such as bacterial virulence, mycobacterial growth, and antigenic variation (8). For example, two PPE proteins (PPE31/PPE68) and one PE (PE35) were found to be required for mycobacterial growth *in vivo* during infection of mice (9, 10). A PPE protein from *Mycobacterium avium* (PPE25 ortholog) has been shown to be involved in virulence by hampering vacuole acidification and

This work was supported by National Natural Science Foundation of China Grant 31600747, the youth innovation talents program of the education department of Guangdong province through University Innovation Strong School Project Grants 2016KQNCX141 and Q17024049, National Science and Technology Major Project 2018ZX10731301-004 and 2018ZX10302302-002, and Guangzhou Science and Technology Innovation Committee Grant 201804010317. The authors declare that they have no conflicts of interest with the contents of this article.

This article contains Figs. S1 and S2.

[1] Both authors contributed equally to this work.

[2] To whom correspondence may be addressed. E-mail: yalw135@126.com.

[3] To whom correspondence may be addressed. Tel.: 86-21-5163-0587; Fax: 86-21-5163-0587; E-mail: yingxu2520@fudan.edu.cn.

[4] The abbreviations used are: MTB, *M. tuberculosis*; Th, helper T cell; DC, dendritic cell; TB, tuberculosis; CD, cluster of differentiation; MHC, major histocompatibility complex; JNK, c-Jun N-terminal kinase; TNF, tumor necrosis factor; IL, interleukin; TLR, Toll-like receptor; IFN, interferon; RORγt, RAR-related orphan receptor C; BCG, bacillus Calmette-Guérin; PPD, purified protein derivative; Ab, antibody; MAPK, mitogen-activated protein kinase; p-p38, phosphorylated p38; p-JNK, phosphorylated JNK; Ag, antigen; OVA, ovalbumin; Treg, regulatory T; casp-1, caspase-1; Z, benzyloxycarbonyl; fmk, fluoromethyl ketone; GM-CSF, granulocyte-macrophage colony-stimulating factor; rIL-4, recombinant mouse interleukin-4; p-ERK, phosphorylated extracellular signal–regulated kinase; PE, phycoerythrin; rBCG, recombinant BCG; MFV, mean fluorescence value; DDA, dimethyldioctadecylammonium; rhIL-1β, recombinant human IL-1β.

phagosome-lysosome fusion in macrophages (11). In particular, a series of PE/PPE proteins (such as PPE18, PPE41, and PE_PGRS33) have been linked to the rich source of B- and T-cell epitopes and the presence of antigenic diversity, either in the form of whole recombinant proteins or as individual peptides (12–14). Many PE/PPE antigens are exported or secreted via the type VII secretion systems that are actively involved in pathogenesis and antigenic variability (15). In this context, the cell surface–associated or extracellular localization of PE/PPE proteins is likely linked to their remarkable immunogenicity (12). Additionally, the duplication, homologous recombination, or random insertion of the *pe*/*ppe* genes throughout the MTB genome may lead to substantial degrees of variability in the expression profiles during different phases of infection, possibly hinting at their diverse functions (16). Moreover, the highly immunogenic nature of PE/PPE immunogens is essentially driven by a substantial degree of direct or cross-reactivities in the elicited T cells, which results from the sequence homologies among the PE/PPE family proteins (7). However, this also begs the question of whether the conserved immunogenicity of the PE/PPEs antigens benefits the pathogen. As reported by others, PE/PPE proteins also may contribute to immune evasion by overwhelming the adaptive immune response or inducing robust anti-inflammatory responses (13, 17).

The establishment of a protective response against mycobacterial infections involves different Th1-related cytokines (18). Deficiency of genes encoding Th1-related cytokines increases the susceptibility to MTB challenge in mice and humans (19, 20). DCs play a key role in the initiation and instruction of adaptive immunity. Naïve DC response is programmed toward Th1 priming and controlling the magnitude of the Th1 immune response toward mycobacterial antigens (21). The PE/PPE proteins have been assumed to modulate the immune-effector functions of antigen-presenting cells (6); however, there are few reports deciphering the detailed mechanisms of interaction of PPE antigens with DCs. Thus, functional characterization of the effects of PE/PPE proteins on DC activation will provide insights into mycobacterial immunity.

PPE60 was previously identified in the cell-envelope fraction by MS and exhibited strong humoral reactivity with PPD^+ but not PPD^- individuals (22, 23). The expression of this protein was observed in MTB H37Rv-infected guinea pig lungs at 90 days (24), indicating that PPE60 protein could be necessary for long-term persistence of MTB during infection. Recently, PPE60 antigen has been shown to consistently and significantly induce the expansion of effector $CD4^+$ T-cells subsets, resulting in secretion of interferon (IFN)-γ and reduction of bacterial burdens in mice (25). Additionally, as a component of TB fusion protein vaccine ID87, this antigen induced antituberculosis protective responses (26). The surface localization of PE/PPE proteins might enable the bacteria to interact with the molecules of host innate immune pathways (17, 27). Here, we determined the effects of PPE60 on DC maturation and the mechanism of regulation of host immunity in turn, offering detailed insights into the immune mechanisms underlying the specific potential of PE/PPE proteins as protective immunogens.

Results

PPE60 is associated with the cell wall and is exposed on the cell surface

To investigate the role and localization of the PPE60 protein, the *PPE60* gene from MTB H37Rv was cloned into the expression vector pRSFDuet-1, and the vector was transformed into *Escherichia coli* to express the target protein with a His_6 tag as described under "Materials and methods." The cell lysate and the purified recombinant protein were analyzed by SDS-PAGE and Western blotting using anti-PPE60 antibody (Ab). As shown in Fig. 1*A*, the Coomassie Blue staining showed the expression of the target protein at the expected molecular mass (~39 kDa), which was confirmed by Western blot analysis with anti-PPE60 Ab (Fig. 1*B*). In addition, a recombinant BCG strain expressing the PPE60 protein was developed as described under "Materials and methods." As expected, expression of the PPE60 protein was detected in the cell lysate of the recombinant BCG strain by immunoblotting with anti-PPE60 Ab, whereas it was not detected in the lysates of the wildtype (WT) BCG or rBCG-pMV261 (Fig. 1*C*).

Next, cell fractionation experiments were performed in MTB H37Rv and the recombinant BCG-PPE60 strain. PPE57 is known to be exposed on the cell surface and therefore was used as a positive control (28). The PPE60 protein was detected in the cell wall fraction by immunoblot analysis, whereas Rv2145c (a cytoplasmic protein) was only present in the cytoplasm, indicating that, similarly to PPE57, PPE60 is associated with the cell wall (Fig. 1*D*). To further query the cell-surface localization of PPE60, proteinase K and trypsin degradation assays were carried out on whole recombinant BCG-PPE60 cells followed by Western blot analysis. As expected, PPE60 was degraded by proteinase K and trypsin in just 20 min, whereas the cytoplasmic Rv2145c was not digested at all (Fig. 1*E*). Together, these results demonstrate that PPE60 is likely to be exposed on the cell surface.

PPE60 induces maturation of DCs

DC maturation plays a crucial role in priming adaptive immune responses, and it is critically dependent on the cognate interaction between costimulatory molecules on DCs and the associated ligands on T cells (21). Therefore, we investigated whether PPE60 induced DC maturation by measuring the expression levels of major histocompatibility complex (MHC) classes I and II and costimulatory molecules, including CD80 and CD86, in the presence of 1, 5, or 10 μg/ml PPE60 or 5 μg/ml Pam3CSK4. Analysis of flow cytometry showed that PPE60 stimulation enhanced the expression of costimulatory molecules on DCs in a dose-dependent manner (Fig. 2*A*).

Mature DCs secrete a variety of cytokines that influence T-cell polarization. In this regard, we determined whether PPE60 induced the production of inflammatory and regulatory cytokines by priming an innate immune response in DCs. As shown in Fig. 2*B*, the levels of TNFα, IL-6, IL-8, and IL-1β were significantly higher in PPE60-stimulated DCs compared with untreated DCs, which only produced a small amount of these cytokines. Additionally, the levels of IL-12 p70 and IL-23 p19 increased significantly in PPE60-stimulated DCs in a dose-de-

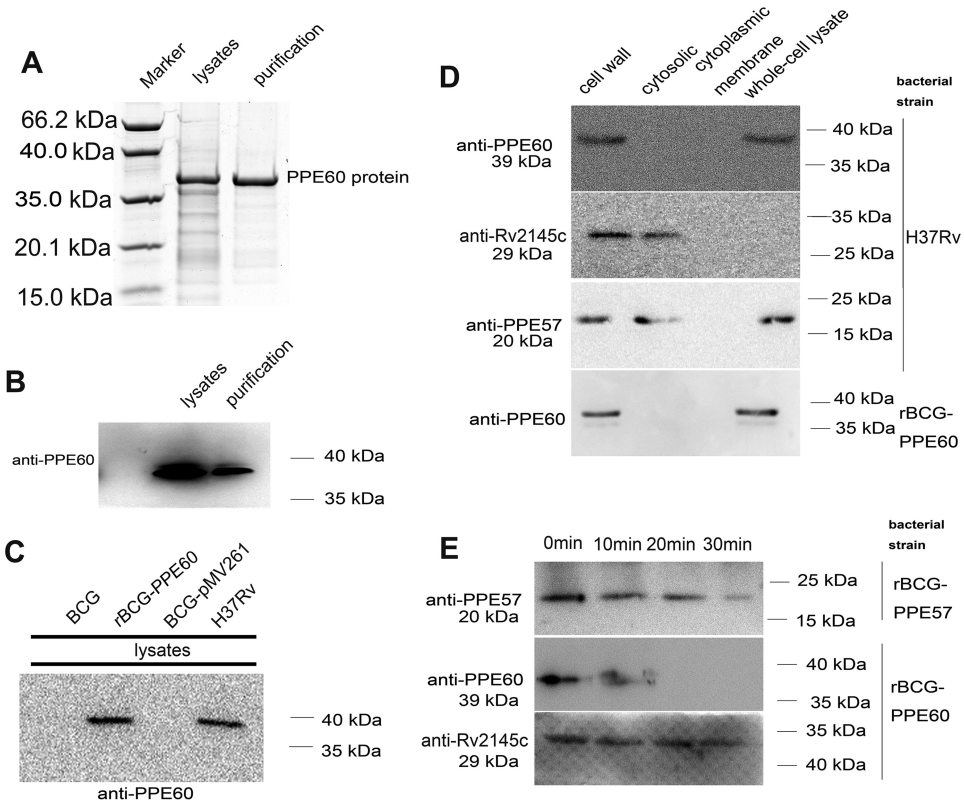

Figure 1. PPE60 is localized to mycobacterial cell surface. *A*, sample from lysates and the purified recombinant protein were examined by Coomassie Blue staining. *B*, Western blotting was used to analyze PPE60-His_6 protein expression with anti-His antibody. *C*, PPE60 expression in recombinant BCG was detected by Western blot analysis. *D*, the localization of PPE60 protein was examined by Western blotting with anti-PPE60 antibody. The expression of Rv2145c (as a cytosolic control) and PPE57 protein (as a positive control) was also analyzed with anti-Rv2145c or anti-PPE57Ab, respectively. *E*, rBCG-PPE60 and rBCG-PPE57 were treated with proteinase K for 0–30 min. PPE60 expression in each sample was detected by immunoblotting using anti-PPE60 Ab. Rv2145c and PPE57 were examined as controls.

pendent manner, whereas the levels of IL-10 were not altered (Fig. 2*C*). We also investigated the intracellular production of IL-12 p70 and IL-10. Compared with untreated DCs, a higher percentage of PPE60-treated DCs were IL-12 p70–positive, whereas negligible change was observed in the number of IL-10–positive cells (Fig. 2*D*). IL-12 p70 and IL-23 p19 are associated with the development of Th1 and Th17 responses (29). In contrast, PPE60 could not induce IFN-β production (Fig. S1), which is also essential for DC maturation and T cell priming. Therefore, these results strongly suggest that PPE60 is a potent effector of DC maturation, inducing the secretion of proinflammatory cytokines that could eventually prime Th1 and Th17 immune responses.

PPE60 is a ligand for Toll-like receptor 2 (TLR2)

TLRs recognize pathogen-associated molecular patterns from mycobacterial cell components and activate cellular immune responses. Many other PPE proteins (such as PPE18, PPE26, and PPE57) have been shown to bind to TLR2 (28, 30, 31). Thus, to determine whether PPE60 acted through TLR2 recognition, DCs were incubated with anti-TLR2, anti-TLR4, or IgG isotype control Ab followed by treatment with increasing concentrations of PPE60 for 24 h, and IL-1β production in supernatants was measured by ELISA. PPE60 induced the secretion of IL-1β in DCs treated with anti-TLR4 and anti-IgG but not in cells treated with anti-TLR2 Ab (Fig. 3*A*). Flow cytometry analysis also showed that PPE60 bound to the surface of WT DCs but not to the surface of TLR2$^{-/-}$ cells (Fig. 3*B*). Confocal imaging analysis further confirmed this observation (Fig. 3*C*). Moreover, western blots showed that immobilized PPE60 could pulldown TLR2 (Fig. 3*D*), whereas no band was visible in the control group or the group containing TLR4 (Fig. 3*D*). These findings suggested that PPE60 interacts specifically and predominantly with TLR2. To ascertain if PPE60 induced DCs activation via TLR2, we examined the expression of cell-surface molecules and the production of cytokines in PPE60-stimulated DCs from WT, TLR2$^{-/-}$, and TLR4$^{-/-}$ mice. Both, cell-surface molecule expression (Fig. 3*E*) and inflammatory cytokine production (Fig. 3*F*) were promoted in PPE60-treated WT and TLR4$^{-/-}$ DCs, whereas these effects were significantly abrogated in TLR2$^{-/-}$ DCs. Taken together, these results clearly indicate that PPE60 is a potent TLR2 agonist and induces DC maturation.

PPE60-induced DC activation via MAPK and NF-κB pathways

Activation of TLR2 signaling induces the recruitment of MyD88 and the subsequent activation of the MAPKs and NF-κB signaling pathways, which are critical for DC maturation (32). Therefore, we analyzed whether PPE60 induced DC activation via the MAPK and NF-κB pathways. To this end, DCs were incubated with culture medium, 10 μg/ml PPE60, 1 μg/ml lipopolysaccharide (LPS), or 5 μg/ml Pam3CSK4, and the phosphorylation status of MAPKs and the nuclear translocation of NF-κB p65 were evaluated by Western blot analysis.

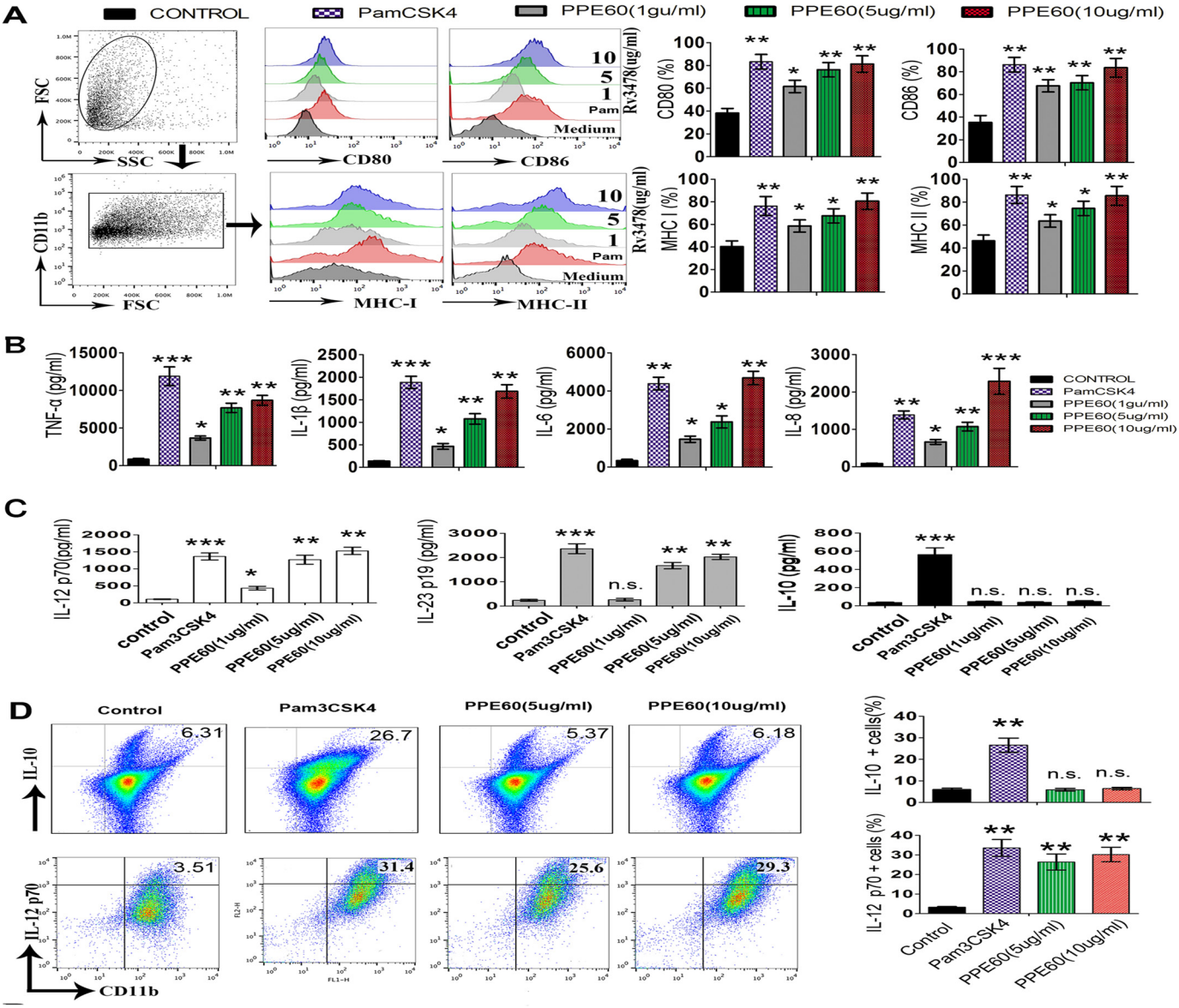

Figure 2. PPE60 functionally induces DC maturation. *A*, immature DCs were treated for 24 h with IL-4 and GM-CSF alone (control); or IL-4, GM-CSF, and 1, 5, or 10 μg/ml PPE60; or IL-4, GM-CSF, and 5 μg/ml Pam3CSK4. DCs were labeled with anti-CD80, anti-CD86, anti-MHC-I, or anti-MHC-II. Flow cytometry was used to analyze the expression of surface markers on DCs. The percentage of positive cells is showed in each panel. *B* and *C*, the production of IL-1β, TNFα, IL-6, IL-8, IL-10, IL-12 p70, and IL-23 p19 was measured via ELISA. *D*, intracellular staining analysis of IL-10 and IL-12 p70 in DCs. Each panel represents the percentage of positive cells. Values are expressed as mean ± S.D. *Error bars* represent S.D. The data shown are representative of two to three independent experiments. *, $p < 0.05$; **, $p < 0.01$; ***, $p < 0.001$, as compared with control group. No significance is marked as *n.s.* *FSC*, forward scatter; *SSC*, side scatter.

As shown in Fig. 4*A*, PPE60 triggered a strong phosphorylation of p38 and JNK in DCs. Similar results were observed by confocal microscopy analysis of cells stained with Abs specific to p-p38 and p-JNK (Fig. 4*B*). Additionally, PPE60 induced a robust nuclear translocation of NF-κB p65 (Fig. 4*A*).

To determine the functional roles of MAPKs and NF-κB signaling in DC activation induced by PPE60, pharmacological inhibitors were used, and inflammatory cytokine secretion and costimulatory molecular expression were evaluated following PPE60 stimulation. Specifically, DCs were pretreated with a p38 inhibitor (SB203580; 30 μM), a JNK inhibitor (SP600125; 50 μM), or an NF-κB inhibitor (Bay11-7082) for 1 h prior to stimulation with PPE60 (10 μg/ml). Predictably, these inhibitors significantly abrogated the PPE60-induced expression of the costimulatory molecules CD80 and CD86 and MHC-I (Fig. 4*C*) and the production of proinflammatory cytokines such as TNFα, IL-6, and IL-12 p70 (Fig. 4*D*). These findings suggest that the MAPKs and NF-κB pathways are essential for PPE60-induced DC maturation.

PPE60 enhances MHC-II expression and Ag processing by DCs in a TLR2-dependent manner

We subsequently studied whether PPE60 affects MHC-II expression. To this end, DCs were treated with only medium, PPE60, or IFN-γ, and MHC-II expression was examined using flow cytometry. After 48-h treatment, a 2.92-fold increase in MHC-II expression was observed in DCs treated with IFN-γ, whereas the expression levels remained low in DCs incubated with only medium. Similarly, a 2.36-fold increase in MHC-II expression was observed in DCs treated with PPE60 compared

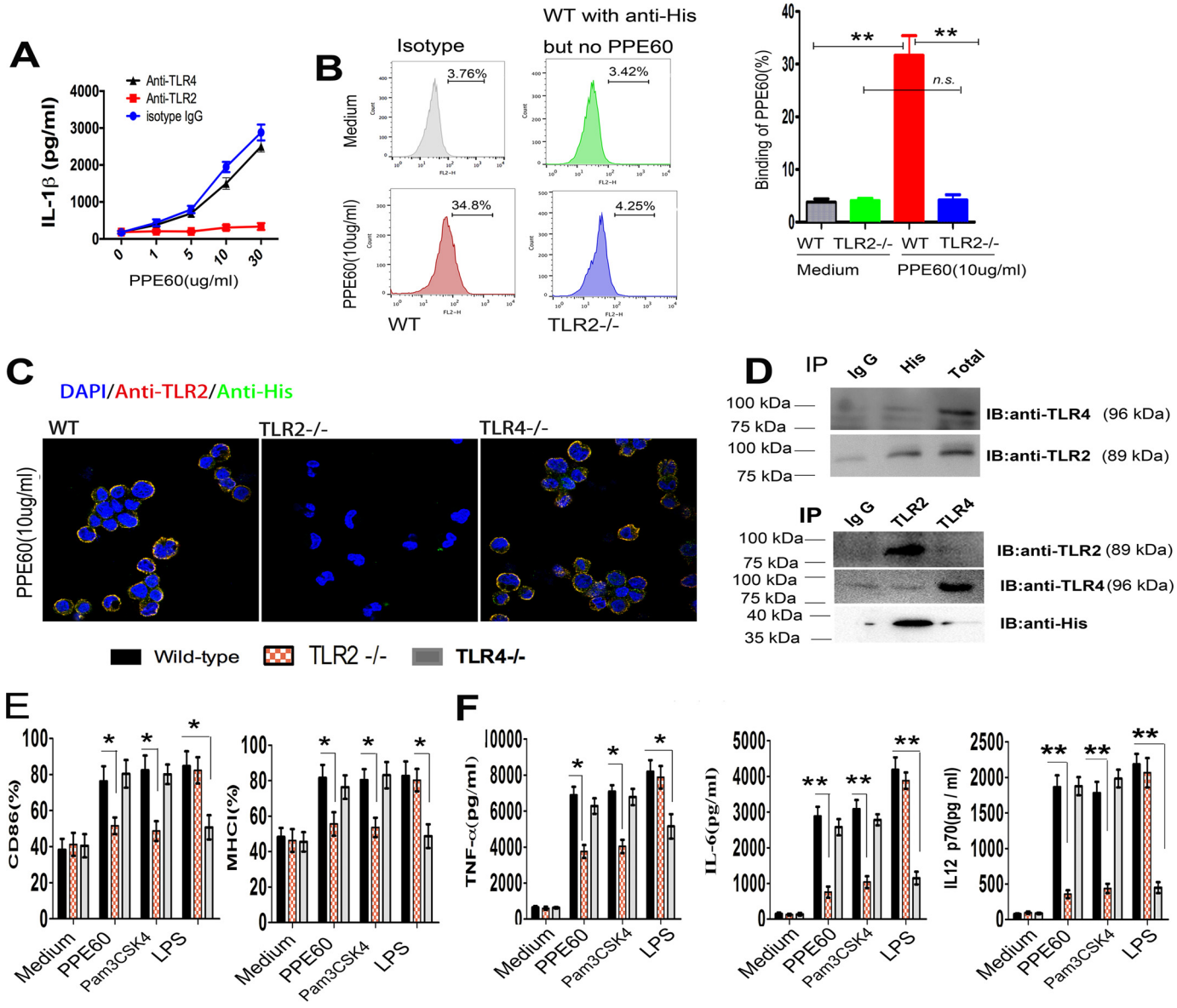

Figure 3. PPE60 induces DC activation via TLR2. *A*, the quantities of IL-1β in the culture supernatant were determined using ELISA. *B*, the interaction of PPE60 with DCs was evaluated by flow cytometry. Representative flow cytometry plots are shown on the *left*. *C*, fluorescence intensities were detected by confocal microscopy to determine the binding of PPE60 to TLR2. *Scale bar*, 50 μm. *D*, immunoprecipitation (*IP*) with anti-His and immunoblotting (*IB*) with anti-TLR2 or anti-TLR4 Ab. The target proteins were visualized using immunoblotting with anti-TLR2 or anti-TLR4 Ab. The total shown represents the mean total cell lysates (input). *E* and *F*, DCs from WT, TLR2$^{-/-}$, and TLR4$^{-/-}$ mice were stimulated for 24 h with 10 μg/ml PPE60, 100 ng/ml LPS, or 5 μg/ml Pam3CSK4. *E*, CD86 or MHC class I expression on DCs was detected by staining using flow cytometry. *F*, the levels of TNFα, IL-6, and IL-12 p70 were analyzed using ELISA. Values are expressed as mean ± S.D. *Error bars* represent S.D. *, $p < 0.05$; **, $p < 0.01$, as compared with control group. No significance is marked as *n.s.*

with treatment with only medium. Coincubation with both PPE60 and IFN-γ increased the expression of MHC-II 3.7-fold (Fig. 5*A*).

Next, we investigated the role of TLR2 in MHC-II expression induced by PPE60. DCs from C57BL/6 or TLR2$^{-/-}$ mice were treated with or without PPE60 for 24–48 h, and MHC-II expression was examined by flow cytometry. PPE60 promoted MHC-II expression in DCs from both types of mice; however, MHC-II expression was lower in TLR2$^{-/-}$ mice than in C57BL/6 mice after 48-h incubation (Fig. 5*B*), indicating that PPE60 may enhance MHC-II expression in a TLR2-dependent manner.

Finally, we examined whether PPE60 also affects the Ag-processing ability of DCs. To this end, DCs from WT or TLR2$^{-/-}$ mice were treated with or without PPE60 for 24 h in the presence of IFN-γ followed by exposure to OVA(323–339) for 3 h and coculturing with DOBW T hybridoma cells for 24 h at a ratio of 1:10. IL-2 production was measured by the CTLL-2 assay as described as described under "Materials and methods." As shown in Fig. 5*C*, exposure of DCs to PPE60 enhanced IL-2 production with a substantial increase observed in the presence of 500 ng/ml OVA(323–339) and the maximum obtained with 1000 ng/ml OVA(323–339) (Fig. 5*D*). However, the increased production of IL-2 was attenuated in TLR2$^{-/-}$ DCs compared with that in WT and TLR4$^{-/-}$ cells (Fig. 5*D*). These results demonstrate that exposure of DCs to PPE60 increases IL-2 production from T cells, indicating that PPE60 promotes MHC-II processing of OVA(323–339) in a TLR2-dependent manner.

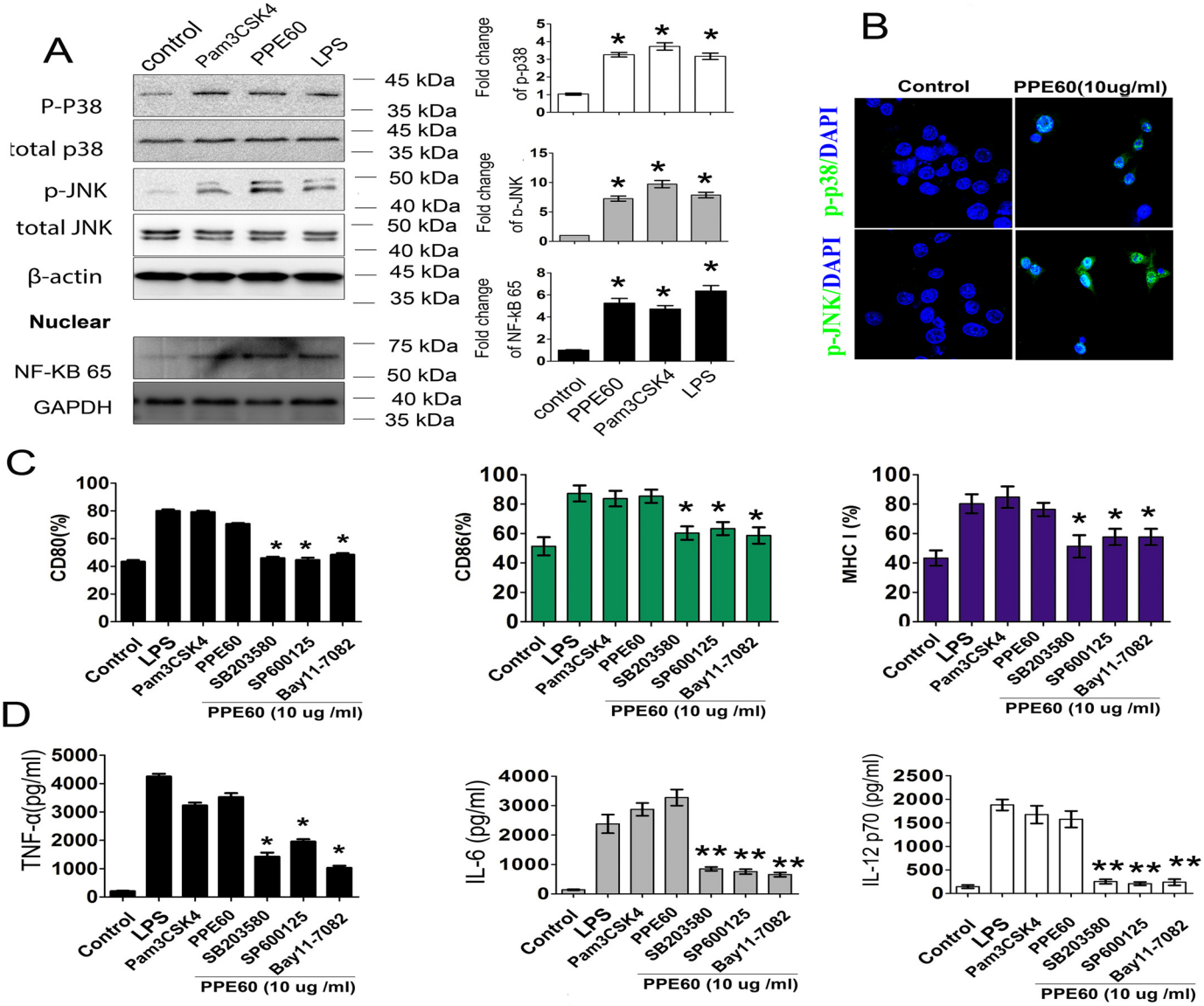

Figure 4. PPE60 triggered DC maturation dependent on the activation of MAPKs and NF-κB signaling. *A*, Western blotting was used to detect target proteins using antibody specific to p38, p-p38, JNK, p-JNK, or NF-Kb p65. *B*, immunofluorescence microscopy analysis of the levels of phosphorylated p38 and JNK in DCs treated with PPE60 for 1 h. *Scale bar*, 50 μm. *C* and *D*, DCs were treated for 1 h with pharmacological inhibitors of p38 (SB203580; 20 μM), JNK (SP600125; 10 μM), and NF-κB (Bay11-7082; 20 μM) or with DMSO (as a blank control) followed by treated with PPE60 (10 μg/ml) for 24 h. *C*, flow cytometry was used to examine CD80, CD86, and MHC-I expression. *D*, the levels of TNFα, IL-6, and IL-12 p70 in the supernatant were detected using ELISA. Values are expressed as mean ± S.D. *Error bars* represent S.D. The data shown are representative of two to three independent experiments. *, $p < 0.05$; **, $p < 0.01$, as compared with control group.

To further validate this conclusion, DCs pretreated with IgG isotype control, anti-TLR2, or anti-TLR4 Ab for 18 h were incubated in the presence or absence of 10 μg/ml PPE60 and then cocultured with splenic $CD4^+$ T cells from mice immunized with PPE60. We found that production of IL-2 significantly increased by IFN-γ or PPE60 stimulation (Fig. 5*E*), but it was abrogated at 48 h in DCs pretreated with anti-TLR2 but not in DCs pretreated with anti-TLR4 or the isotype control Ab (Fig. 5*E*). Additionally, DCs from C57BL/6 mice or $TLR2^{-/-}$ mice were preincubated with or without 10 μg/ml PPE60 and then cocultured with splenic $CD4^+$ T cells from mice immunized with PPE60 protein. The release of IL-2 was significantly higher in splenic $CD4^+$ T cells cocultured with DCs than that in T cells cocultured with $TLR2^{-/-}$ DCs (Fig. 5*F*). In contrast, we did not observe any changes in the release of IL-2 in splenic $CD4^+$ T cells cocultured with DCs compared with those cells cocultured with $TLR2^{-/-}$ DCs (Fig. 5*G*). These results indicate that PPE60 promotes the processing of multiple antigens. Specifically, our results suggest that PPE60 promotes MHC-II expression and Ag processing via a TLR2-dependent mechanism, potentially resulting in enhanced MHC-II presentation, as demonstrated by the increased IL-2 levels, as it is well-known that specific MHC-II peptide presentation to $CD4^+$ T cells occurs before the production of IL-2 (33, 38).

PPE60-treated DCs induce naïve T-cell expansion and Th1/Th17 differentiation

DCs can efficiently prime naïve T cells to induce a Th1/Th17 response. Therefore, we investigated whether the PPE60-enhanced MHC-II expression in DCs affected their ability to

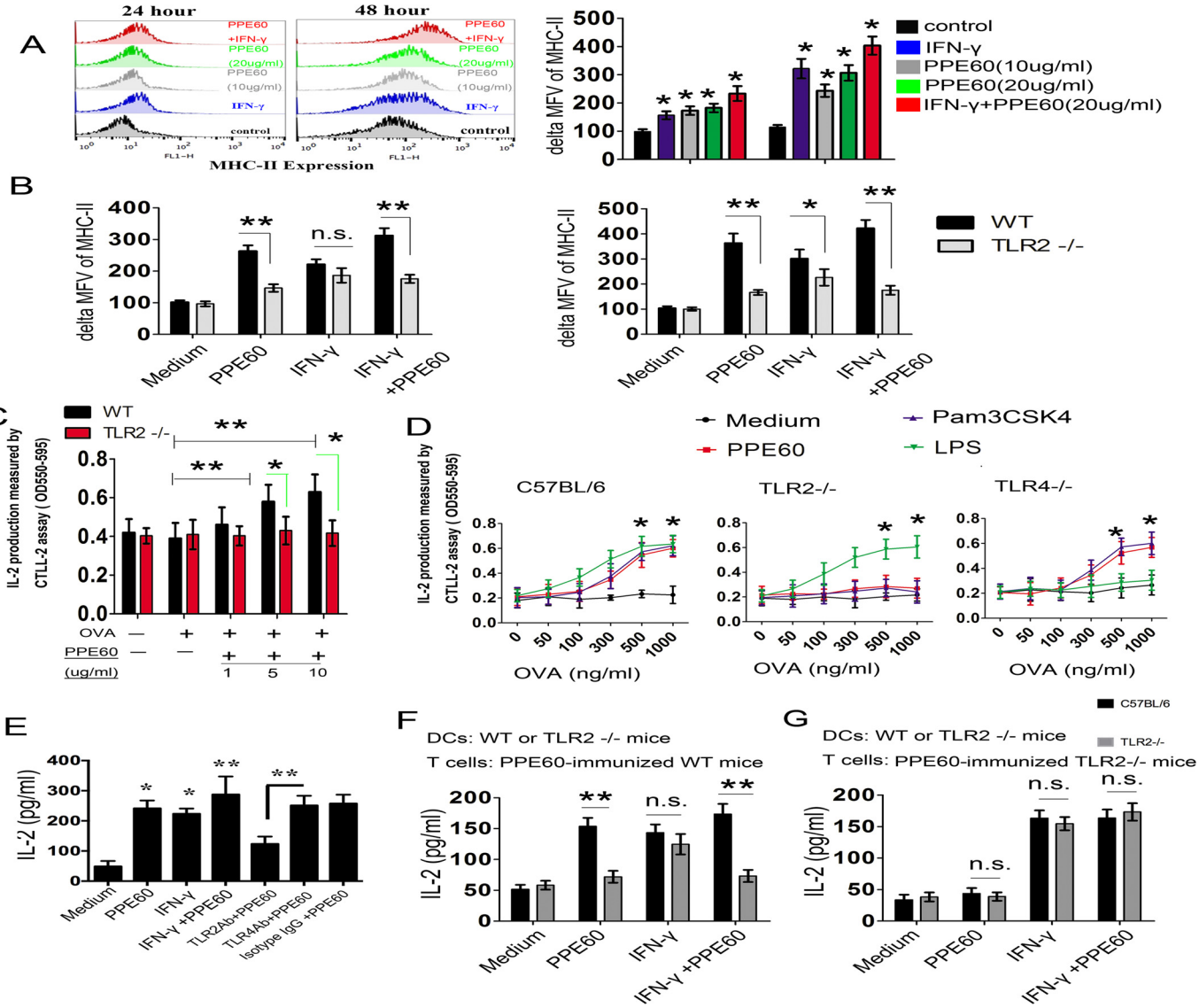

Figure 5. PPE60 enhances MHC-II expression and Ag processing via TLR2. *A*, the expression of MHC-II was determined using flow cytometry. Representative flow cytometry plots are shown on the *left*. *B*, PPE60 promotes MHC-II expression via TLR2 in DCs. In *A* and *B*, ΔMFV was determined as the MFV of cells labeled with MHC-II Abs minus the MFV of cells stained with isotype Abs. *C*, DCs were treated for 24 h with or without the indicated concentrations of PPE60 in the presence of 15 ng/ml IFN-γ. Cells were then stimulated with 800 ng/ml OVA(323–339) for 3 h. DCs were finally cocultured with DOBW T-hybridoma cells for 24 h at a ratio of 1:10. IL-2 production in the supernatants was detected using a CTLL-2 assay. *D*, DCs prepared from WT, TLR2$^{-/-}$, or TLR4$^{-/-}$ mice were incubated with 10 μg/ml PPE60 in the presence of IFN-γ (15 ng/ml) for 24 h. Cells were then treated for 3 h with the indicated concentrations of OVA(323–339). Antigen processing was determined with DOBW T-hybridoma cells as mentioned above. *E*, DCs were treated with Ab specific to isotype IgG, TLR2, or TLR4 for 18 h and then stimulated with or without 10 μg/ml PPE60 in the presence of IFN-γ (15 ng/ml) for 24 h. PPE60 Ag–specific CD4$^+$ T cells were then cocultured with those DCs for 48 h at a ratio of 10:1 (T cells:DCs). The level of IL-2 was detected using ELISA. *F* and *G*, DCs isolated from WT and TRL2$^{-/-}$ mice were treated with or without 10 μg/ml PPE60 in the presence of IFN-γ (15 ng/ml) for 24 h. Then PPE60-specific CD4$^+$ T cells from PPE60-immunized C57BL/6 (*F*) or TLR2$^{-/-}$ mice (*G*) were incubated with DCs for 48 h. IL-2 secretion was determined as mentioned. The data shown are the mean values ±S.E. *Error bars* represent S.E. Data are representative of two to three independent experiments. *, $p < 0.05$; **, $p < 0.01$, as compared with control group. No significance is marked as *n.s.*

polarize T cells toward a Th1/Th17 response. To this end, we performed syngeneic mixed lymphocyte reaction assays using antigen-specific T cells from antigen 85B (Ag85B)-immunized mice. DCs stimulated with PPE60 elicited significant proliferation of splenocytes (Fig. 6*A*). CD4$^+$ T cells cocultured with PPE60-pretreated DCs induced significantly more IFN-γ than those primed with unstimulated DCs or with LPS-stimulated DCs (Fig. 6*B*). We did not observe any changes in the levels of IL-4 secretion regardless of PPE60 treatment. In addition, high levels of IL-17A, a Th17-type cytokine, were detected in splenocytes primed with PPE60-stimulated DCs compared with those cultured with untreated DCs or LPS-treated DCs (Fig. 6*B*). The differentiation of CD4$^+$ T splenocytes was further tested by intracellular cytokine staining followed by flow cytometry. Intracellular staining of Th17 lymphocytes for IL-17A (Fig. 6*C*) and the Th17-specific RORγt (Fig. 6*D*) significantly increased. An enhanced production of IFN-γ and T-bet was also observed, whereas no increase in the production of IL-4 and GATA-3 was detected (Fig. 6, *C* and *D*). Moreover, no changes in the levels of Foxp3 and Treg lymphocytes were observed (Fig. 6*E*). Taken together, these results show that PPE60-stimulated DCs promote the differentiation of Th1/Th17 responses.

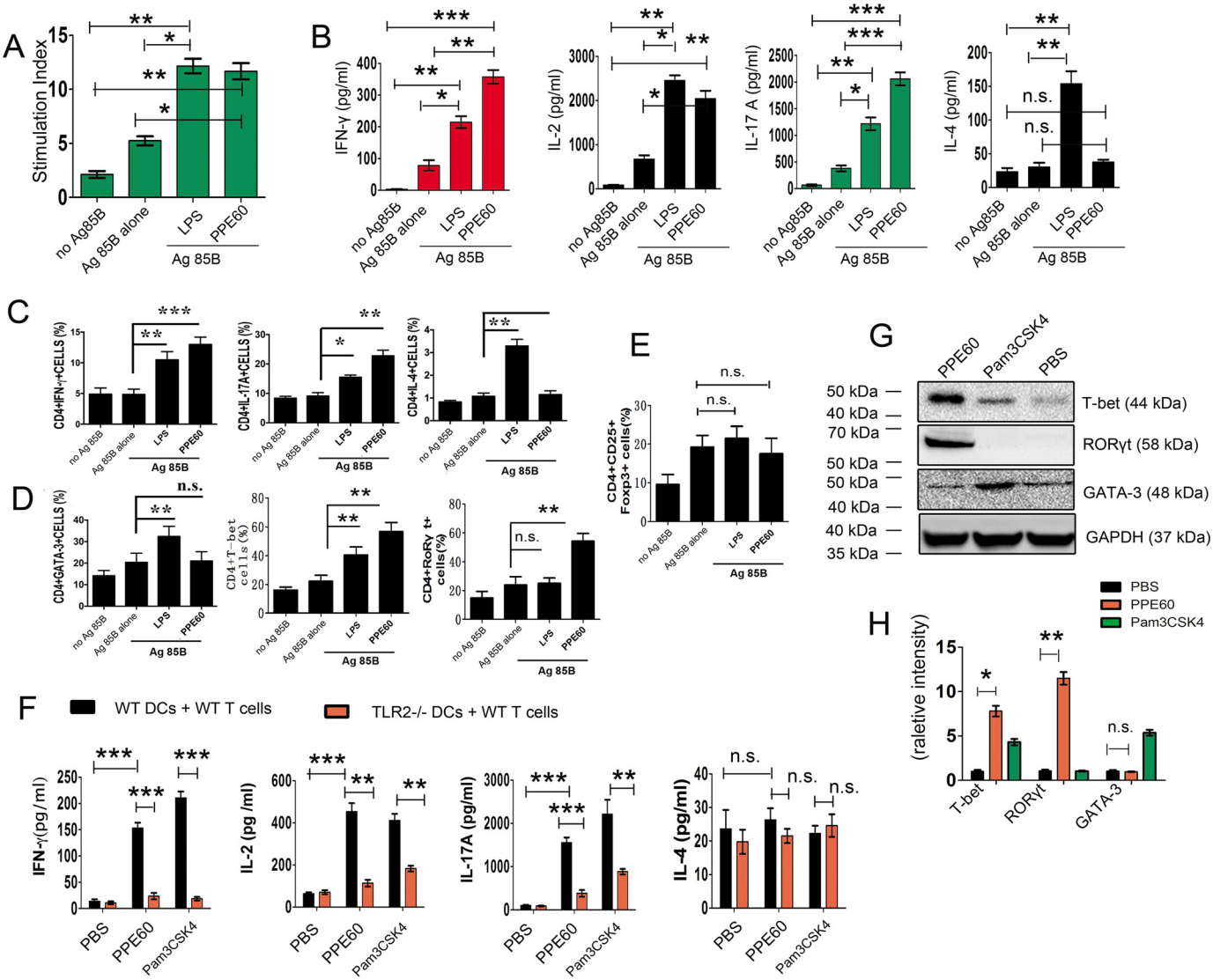

Figure 6. PPE60-stimulated DC promotes the differentiation of Th1 and Th17 cells. In *A–E*, Ag85B-specific $CD4^+$ T cells were prepared, using a MACS column, from C57BL/6 mice immunized with Ag85B. DCs from C57BL/6 mice were stimulated with 10 μg/ml PPE60 or 100 ng/ml LPS for 24 h. Then T cells were cocultured with DCs at a ratio of 10:1 for 96 h followed by a pulse with Ag85B (10 μg/ml). *A*, cells were pulsed with 0.5 μCi of tritiated thymidine for 16 h, harvested, and counted. Stimulation indices were obtained by dividing cpm obtained by the sum of cpm obtained for corresponding DCs plus T cells alone. *B*, the levels of IFN-γ, IL-2, IL-4, and IL-17A were determined using ELISA in the culture supernatants. Cytokine production in $CD4^+$ T cells (*C*) and the expression of GATA-3, T-bet, and RORγt (*D*) and Foxp3 (*E*) were finally detected using intracellular staining. *F* and *G*, $CD4^+$ splenocyte T cells from PPE60-immunized C57BL/6 mice and DCs from C57BL/6 and $TLR2^{-/-}$ mice were stimulated with 10 μg/ml PPE60, 100 ng/ml LPS, or 5 μg/ml Pam3CSK4 for 24 h. Then T cells were cocultured with DCs at a ratio of 10:1 for 3 days. *F*, graphic depiction of the levels of IFN-γ, IL-2, IL-17A, and IL-4 in the culture supernatants in each group as determined by ELISA analysis. *G*, the levels of T-bet, GATA-3, and RORγt expression were determined by Western blotting. *H*, densitometric analysis of the Western blot in *G*. The data shown are the mean values ±S.E. *Error bars* represent S.E. The data shown are representative of two to three independent experiments. *, $p < 0.05$; **, $p < 0.01$; ***, $p < 0.001$, as compared with control group. No significance is indicated by *n.s.*

To investigate the role of TLR2 in Th1 and Th17 responses induced by PPE60, DCs isolated from C57BL/6 mice or $TLR2^{-/-}$ mice were pretreated with PPE60, Pam3CSK4, or PBS. Cells were then cocultured for 48 h with $CD4^+$ T cells from PPE60-immunized C57BL/6. ELISA analysis revealed that the secretion of cytokines IFN-γ, IL-2, and IL-17 production and the expression of T-bet and RORγt proteins were more enhanced in $CD4^+$ T cells primed with PPE60-pulsed DCs than those cocultured with PBS-treated DCs. However, DCs from $TLR2^{-/-}$ mice failed to induce these T-cell responses after PPE60 stimulation (Fig. 6, *G* and *H*). These results suggest that PPE60-exposed DCs induce a Th1/Th17 response via TLR2.

PPE60 activates the NLRP3 inflammasome in DCs dependent on TLR2

MTB components recognized by pattern recognition receptors activate the NLRP3 inflammasome and thereby promote IL-1β secretion (34, 35). However, few MTB antigens are known to be involved in inflammasome activation. Previously, we found that PPE60 induced the secretion of IL-1β in DCs. Therefore, we asked whether PPE60 could modulate NLRP3 inflammasome activation. DCs were stimulated with PPE60 (10 μg/ml) or ESAT-6 protein (5 μg/ml; positive control) for 18 h, and the fluorescence intensity of NLRP3 (green) and caspase-1 (casp-1) (red) on cells was analyzed by confocal microscopy.

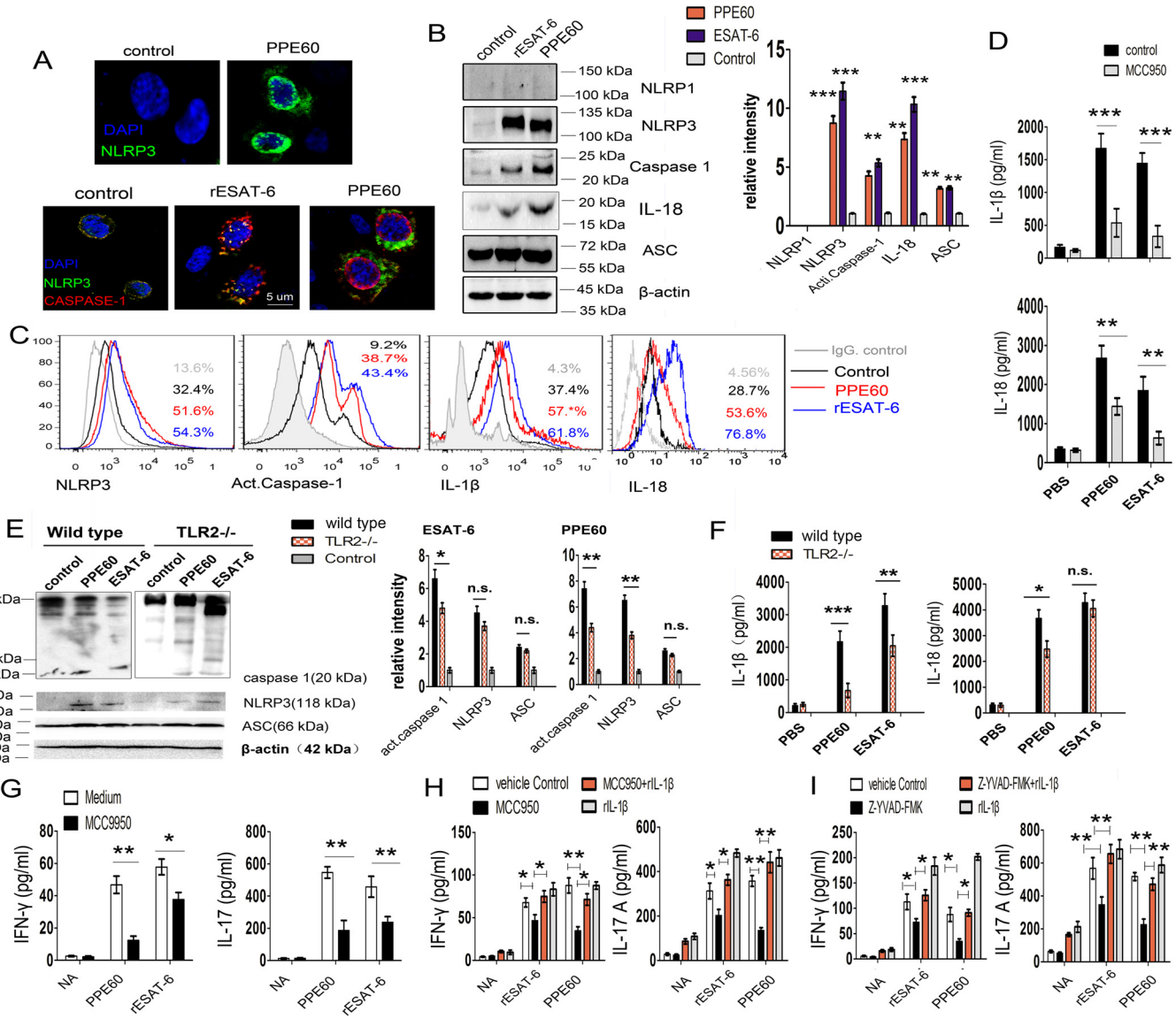

Figure 7. PPE60 induces NLRP3 inflammasome activation in DCs. DCs were stimulated with purified ESAT-6 (5 μg/ml; as a positive control) or PPE60 (10 μg/ml) for 18 h. *A*, representative fluorescence intensity for NLRP3 (*green*) and caspase-1 (*red*) on PPE60-activated DCs. *B*, NLRP3, caspase-1, IL-18, and ASC immunoblotting on PPE60-activated DCs. *C*, NLRP3, activated caspase-1, IL-1β, and IL-18 proteins were analyzed by flow cytometry. *D*, levels of IL-1β and IL-18 were measured via ELISA in the presence or absence of MCC950. *E* and *F*, DCs (1.0×106 cells/well) isolated from C57BL/6 or TLR2$^{-/-}$ mice were treated for 18 h with PPE60 or ESAT-6 (as a control). *E*, Western blotting was used to determine the expression of NLRP3, casp-1, IL-18, and ASC proteins. *F*, levels of IL-1β and IL-18 were measured via ELISA. *G–I*, ESAT-6 –treated or PPE60-treated DCs were simultaneously incubated with 10 mmol/ml MCC950 (CP-456773) or 5 mmol/ml Z-YVAD-fmk (S810202) in the presence or absence of 50 units/ml rhIL-1β for 18 h. CD4$^+$ T cells were cocultured with DCs at a 1:10 ratio (DC:T cells) for 48 h. *G*, IFN-γ and IL-17 production in CD4$^+$ T cells cocultured with DCs, which were treated with or without MCC950 (*H*) and with or without rhIL-1β. *I*, levels of IFN-γ and IL-17 were measured via ELISA in the presence of caspase-1 inhibitor Z-YVAD-fmk with or without rhIL-1β addition. The data shown are the mean values $\pm$S.E. *Error bars* represent S.E. The data shown are representative of two to three independent experiments. *, $p < 0.05$; **, $p < 0.01$; ***, $p < 0.001$, as compared with control group. No significance is indicated by *n.s. NA* indicates nonactivated.

We found that expression of the NLRP3 and active casp-1 was significantly up-regulated (Fig. 7*A*). Consistent with this observation, immunoblot analysis and flow cytometry showed that PPE60 indeed up-regulated the expression of NLRP3 and promoted production of active casp-1 with a subsequent increase in IL-1β and IL-18 generation (Fig. 7, *B* and *C*). IL-18 is part of the NLRP3 inflammasome pathway (36). Moreover, NLRP3 inhibition significantly attenuated IL-1β and IL-18 production in DCs treated with PPE60 (Fig. 7*D*). These results indicate that PPE60 induces the activation of the NLRP3 inflammasome in DCs.

TLR2 uses the MyD88 pathway to prime and activate the NLRP3 inflammasome (37). To determine whether inflammasome activation induced by PPE60 is TLR2-dependent, DCs (1.0×10^6 cells/well) isolated from C57BL/6 or TLR2$^{-/-}$ mice were treated for 18 h with PPE60 or ESAT-6 and then analyzed by Western blotting using anti-NLRP3, anti-casp-1, or anti-ASC Ab. The levels of IL-1β and IL-18 were measured in the medium supernatant. We found that TLR2$^{-/-}$ DCs showed a small amount of NLRP3 expression and active casp-1 activation after stimulation with PPE60 compared with WT DCs (Fig. 7*E*). Consistent with this, priming TLR2$^{-/-}$ DCs with PPE60 failed

to induce IL-1β and IL-18 secretion (Fig. 7*F*). These results indicate that PPE60-induced NLRP3 inflammasome activation may be dependent on TLR2.

IL-1β produced by Ag-presenting cells is involved in maintaining the priming and imprinting effector function of T cells and IFN-γ secretion and IL-17 generation from $CD4^+$ T cells (38). Therefore, it was crucial to examine the effect of PPE60-induced NLRP3 activation on both IL-1β secretion and the generation of Th1 and Th17 cells. DCs were treated with PPE60 in the presence or absence of MCC950 (a specific NLRP3 inhibitor). Then they were cocultured with $CD4^+$ T cells from PPE60-immunized mice. Finally, IFN-γ and IL-17 production was assayed by ELISA. The results showed that NLRP3 inhibition in DCs specifically attenuates IFN-γ and IL-17 production from $CD4^+$ T cells (Fig. 7*G*). Moreover, addition of recombinant IL-1β completely reversed the effect of the NLRP3 inhibitor (Fig. 7*H*). Similarly, IL-17 and IFN-γ secretion was repressed by the Z-YVAD-fmk–mediated reduction of active casp-1 activity (Fig. 7*I*). These results indicate that PPE60 may activate the NLRP3/caspase-1/IL-1β signaling pathway, which is essential for PPE60-induced Th1/Th17 response.

Discussion

PE/PPE proteins are thought to have an important role in pathogenicity and immunogenicity (13). However, the detailed molecular mechanisms through which the PE/PPE proteins favor host–pathogen interactions remain unclear. DCs are crucial for eliciting immune responses to mycobacteria infection through orchestrating distinct Th1/Th17 responses based on the signals they receive (39). Thus, determining the effects of PE/PPE proteins on DCs will likely pave a way for their inclusion in pathogenicity and TB vaccines (25, 38). In this study, we found that PPE60, a representative member of PPE antigens, was surface-exposed. PPE60 effectively induced DC maturation and triggered NLRP3 inflammasome activation. Importantly, PPE60-stimulated DCs polarized T cells toward Th1 and Th17 types. It has been proposed that antigen targets for the rational design of MTB vaccines should contain the following molecular features: good accessibility, excellent ability to activate antigen-presenting cells, and ability to induce Th1/Th17 responses (6). Therefore, this finding makes PPE60 a promising antigen candidate for TB subunit vaccines.

Emerging evidence increasingly supports a critical role for the PE/PPE proteins in the interaction with host components, possibly by modulation of innate immunity and the subsequent adaptive immunity via TLR2 (13). For example, PE_PGRS33 directly interacts with TLR2, thereby inducing cytokine secretion, apoptosis, and necrosis (40). PPE34 preferentially induces the secretion of IL-10 in DCs via TLR2/MAPK signaling and promotes IL-4 and IL-5 release from $CD4^+$ T cells, thus inducing Th2 responses (41). Variants of PE/PPE family members elicit differential effects. PE_PGRS17 and PE_PGRS11 recognize TLR2, induce DC maturation, and polarize naïve T cells toward the Th1 type (42). Here, we found that PPE60 directly bound to TLR2, induced maturation and activation of DCs, and enhanced the ability of DCs to stimulate $CD4^+$ T cells. Thus, these lines of evidence suggest that TLR2 engagement is likely a common property of PE/PPE proteins and that the innate and additive host response to interaction with multiple PE/PPE proteins may be multifaceted and could profoundly impact the course of MTB immunopathology (43).

MHC class II molecules are continuously synthesized in response to MTB infection, during which they are loaded with antigenic peptides in the MHC compartment, thereby priming $CD4^+$ T cells (44). Previously, PE_PGRS47 was found to inhibit MHC class II–restricted antigen presentation by dendritic cells (45). In contrast, PE27 functionally induces DC maturation by up-regulating MHC class II expression and enhances its antigen presentation ability (46). Similarly, in this study, we found that PPE60 enhanced MHC-II expression on the surfaces of DCs and potentially enabled DCs to effectively process Ag and present peptides to $CD4^+$ T cells for recognition as reflected by a significant increase in IL-2 production. It is known that IL-2 production follows from Ag presentation (33). These findings indicate that the suppression or activation of the MHC-II system by PE/PPE antigens may be the molecular basis of immune surveillance during MTB infection. Focusing on ways to provide an optimal MHC-II–restricted antigen presentation to $CD4^+$ T helper cells may be a crucial parameter for optimal and protective adaptive immune response against TB (44).

Th1 and Th17 cell immunity is especially crucial for the control of MTB infection (47). Several studies have revealed the ability of PE/PPE proteins to elicit T-cell responses (12). A cohesive understanding of the capacity of PE/PPE proteins to modulate Th1 responses has yet to be established (27). PPE18 strongly induces the secretion of IL-10, which is known to favor a Th2 immune response (36). PE32 and PPE65 antigens are involved specifically in inducing antimycobacterial host immunity by inhibiting the Th1 immune response (48). Previously, PPE26 and PPE57 were found to effectively drive the Th1 response in a TLR2-dependent manner (28, 30). Additionally, PPE42, a component of the ID83 fusion antigen, enhances the production of IFN-γ and skews the immune response toward a Th1 type (49). However, the effects of PE/PPE proteins on the Th17 response have yet to be determined. In this context, we found that PPE60-activated DCs promoted the secretion of IFN-γ and IL-17 from $CD4^+$ T cells, thereby priming the Th17 response. PPE60-activated DCs secreted significantly more IL-23 p19 than did those stimulated with LPS. IL-23 p19 is crucial for both the IL-17 secretion and Th17 responses to mycobacterial infection (50). Moreover, in the case of PPE60 stimulation, the expression of RORγt was increased, but Foxp3 expression was not. As is well-characterized, RORγt is a transcriptional factor specific to Th17 cells that produce IL-17, whereas Foxp3-related Treg cells secrete IL-10 and favor Th2 cell differentiation (51). It has been speculated that direct or cross-reactivity among the PE/PPE family proteins contributes to immune recognition (27). Thus, this work offers detailed insights into the immune mechanisms underlying the IL-17–producing $CD4^+$ T cell responses induced by PE/PPE antigens.

NLRP3 inflammasome assembly and activation modulate the innate immunity against intracellular pathogens (52). In the case of MTB infection, bacilli specifically activate the NLRP3 inflammasome via the virulence-associated RD1 locus of MTB (35). However, MTB factors and the underlying mechanisms involved in the NLRP3 activation are poorly identified. In this

work, we found that PPE60 likely activated the NLRP3 inflammasome in DCs by augmenting NLRP3 protein expression, active caspase-1 generation, and IL-1β and IL-18 secretion. Importantly, IFN-γ and IL-17 production by $CD4^+$ T cells cocultured with PPE60-stimulated DCs required this activity. Similarly, ESAT-6 protein from MTB stimulates the formation of the NLRP3/ASC/caspase-1 inflammasome complex that is important for IL-1β release (53). Activation of the NLRP3 inflammasome may involve the interaction between ligands and TLRs of DCs (37). ESAT-6 activates the NLRP3/IL-1β pathway dependent on TLR2 in intraocular tuberculosis (54). Here, we observed a significant reduction in generation of caspase-1, NLRP3, IL-1β, and IL-18 in $TLR2^{-/-}$ DCs after PPE60 stimulation compared with those in WT DCs, indicating that PPE60-mediated NLRP3 inflammasome activation may be dependent on TLR2. However, other surface or endosomal receptors could contribute to the activation of the NLRP3 inflammasome (36) because PPE60-stimulated $TLR2^{-/-}$ cells did not completely abrogate the expression of NLRP3, IL-1β, and IL-18 genes. Various mediators transmit the second signal for inflammasome complex assembly. This signal is conferred by intracellular reactive oxygen species, potassium efflux, and lysosomal disruption (36). In this context, we further determined whether the potassium efflux is required for PPE60-indcued inflammasome activation. We found that blockade of ATP-sensitive potassium channels with glibenclamide significantly inhibited the production of NLRP3 and IL-1β in PPE60-treated DCs (Fig. S2). These findings indicate that PPE60-indcued NLRP3 inflammasome activation may require potassium efflux via ATP-sensitive potassium channels.

Taken together, PPE60 acts as a TLR2 agonist and induces DC activation. PPE60-stimulated DCs effectively promoted naïve $CD4^+$ T cells differentiation to produce IFN-γ, IL-2, IL-17A and enhanced the expansion of T-bet and RORγt but not GATA-3, thus inducing Th1 and Th17 responses. Moreover, PPE60-induced activation of the NLRP3 inflammasome is required for this activity. ESAT-6–mediated NLRP3 inflammasome activation contributes to the superior protection afforded by a recombinant BCG strain compared with that seen with conventional BCG vaccination (36). Here, we show that the secretion of IL-1β and IL-18 depends on PPE60-mediated NLRP3, indicating that the incorporation of PPE60-based NLRP3 inflammasome mechanisms that lead to Th1 and Th17 responses should, therefore, also be taken into consideration for TB vaccine development.

Materials and methods

Animals and bacteria

C57BL/6 mice (female, 6–8 weeks old) were purchased from the Center of Laboratory Animal Science of Guangdong (Guangzhou, China). $TLR2^{-/-}$ and $TLR4^{-/-}$ mice (female, 6–8 weeks old) were purchased from Sebiona Biotechnology Co. Ltd. (Guangzhou, China). All mice were kept under specific pathogen-free conditions in the Center of Laboratory Animal Science of Guangdong. All experimental procedures were conducted in accordance with the Guidelines for the Care and Use of Laboratory Animals and approved by the Animal Care and Use Ethical Committee of Fudan University.

Antibodies and reagents

Recombinant mouse granulocyte-macrophage colony-stimulating factor (GM-CSF) and recombinant mouse interleukin-4 (rIL-4) were purchased from JW CreaGene (Gyeonggi, Korea). The fluorescein isothiocyanate (FITC)-annexin V/propidium iodine kit was purchased from R&D Systems (Minneapolis, MN). LPS from *E. coli* O111:B4 was purchased from InvivoGen (San Diego, CA). The T-lymphocyte cell enrichment kit was purchased from Miltenyi Biotec (Auburn, CA). GM-CSF; rIL-4; and ELISA kits for TNFα, IFN-γ, IL-1β, IL-2, IL-4, IL-6, IL-8, IL-10, IL-12 p70, and IL-17A were purchased from BD Biosciences. Anti-PPE60 mouse polyclonal Ab, anti-Rv2145c mouse polyclonal Ab, and anti-PPE57 rabbit polyclonal Ab were from C57BL/6 mouse or rabbit immunized with the appropriate synthetic peptides or protein prepared in our laboratory. Anti-His, rabbit anti-ERK1/2 (sc-94), rabbit anti-p-ERK1/2 (sc-16981-R), rabbit anti-p38 (sc-7149), rabbit anti-p-p38 (sc-17825-R), rabbit anti-JNK (sc-571), rabbit anti-p-JNK (sc-135642), rabbit anti-NF-κB p65 (sc-7178), rabbit anti-β-actin (sc-7210), mouse anti-GAPDH (sc-42724) (all from Santa Cruz Biotechnology, Dallas, TX), and horseradish peroxidase (HRP)-conjugated secondary Abs (Sigma) were used to detect the signaling involved in PPE60-modulated DC function. To determine the expression of surface makers on bone marrow–derived cells, the following Abs were used: FITC-conjugated anti-mouse CD80 (561954), PE-conjugated anti-mouse CD86 (561963), FITC-conjugated anti-mouse I-A/I-E (553623), and PE-conjugated anti-mouse H-2κB (560818) for mouse macrophages (BD Pharmingen). The anti-ASC Ab (70627), anti-NLRP3 Ab (ab4207), anti-IL-1β Ab (ab2105), anti-T-bet Ab (ab92486), anti-GATA-3 Ab (ab199428), active-caspase-1 staining kit (ab219935), anti-caspase-1 Ab (ab1872), anti-Foxp3 Ab (ab36607), anti-RORγt Ab (ab207082), anti-IL-18 Ab (ab71495), and ELISA kits for IL-18 (ab216165) were purchased from Abcam (Cambridge, MA).

Cloning and expression of recombinant PPE60

The *PPE60* gene was amplified from MTB H37Rv genomic DNA by PCR using the following primers: forward, 5′-ATTGAATTCGTGGTGGATTTCGGGGCGTTAC-3′; reverse, 5′-ATTAAGCTTCTATCCGGCGGCCGGTGTG-3′. The PCR product was digested with the restriction enzymes EcoRI and HindIII, subcloned into the expression vector pRSFDuet-1 (Novagen, Madison, WI), and transformed into *E. coli* BL21 (DE3). Transformants were cultured at 37 °C until an A_{600} of 0.4–0.5 followed by induction of PPE60 expression with isopropyl β-thiogalactopyranoside (0.1 mM) overnight at 15 °C. Cells were then harvested and disrupted by sonication. Recombinant PPE60 was purified using HIS-Select® Nickel Affinity Gel (Sigma-Aldrich) as described previously with minor modifications (30) followed by treatment with an Endotoxin Removal Resin (Pierce) according to the manufacturer's instructions. Endotoxin-free recombinant protein samples were dissolved in PBS buffer and frozen at −80 °C. The final concentration of purified PPE60 was 0.85 μg of protein/ml as

quantified using a bicinchoninic acid (BCA) protein assay kit (Pierce). Recombinant PPE60 expression was verified by Western blotting using an anti-PPE60 Ab, and the purity of the samples was evaluated by Coomassie Blue and silver nitrate staining.

Construction of rBCG-PPE60 and rBCG-PPE57

A pMV261 plasmid containing the *PPE60* gene was introduced into the Chinese BCG strain (Pasteur Institute, Shanghai, China) by electroporation. Selected rBCG-PPE60 transformants were grown in Middlebrook 7H9 medium containing 10% oleic acid-albumin-dextrose-catalase and 50 μg/ml kanamycin. The construction of rBCG-PPE57 was performed as described previously (46). Expression of the PPE60 protein or PPE57 protein in the recombinant BCG strain was verified by Western blotting using anti-PPE60 Ab or anti-PPE57 Ab, respectively.

Localization of the PPE60 protein

Subcellular protein fractionation of MTB H37Rv and rBCG-PPE60 was performed as described previously (28, 55, 56). Briefly, bacterial cells were sonicated for 30 s at room temperature in 10-s cycles followed by chilling in an ice bath. The lysates were centrifuged at 11,000 $\times$ *g* for 5 min at 4 °C to precipitate cellular debris and unlysed cells. The resulting supernatant was ultracentrifuged at 27,000 $\times$ *g* for 2 h at 4 °C to collect the cell wall–associated proteins. Next, the supernatant was precipitated at 110,000 $\times$ *g* for 2 h to separate the cytoplasmic membrane (pellet) from the cytosolic fraction (supernatant). Cytosolic proteins were subsequently precipitated by incubation with 10% TCA (v/v) on ice for 30 min and centrifugation for 10 min at 16,000 $\times$ *g* at 4 °C followed by wash with 80% acetone (v/v). The subcellular fractions obtained were analyzed by Western blotting using anti-PPE60 and anti-Rv2145c mouse polyclonal Abs and anti-PPE57 rabbit polyclonal Ab prepared in our laboratory.

The proteinase K degradation assay was used to confirm association of PPE60 to the cell surface as described previously (28). Briefly, selected strains were inoculated in 20 ml of medium at an A_{600} of 0.1 and grown for 14 h. Then cells were washed once in TBS buffer (Tris-HCl, pH 7.5, 150 mM NaCl, 3 mM KCl) and resuspended in 1 ml of the same buffer. Each sample was next treated with 100 μg/ml proteinase K for the indicated times at 37 °C, and the reaction was terminated by adding a protease inhibitor mixture (Roche Applied Science). Samples were boiled for 10 min to allow bacterial lysis and loaded on a polyacrylamide gel in equal amounts. Each sample was finally subjected to Western blotting using anti-PPE60, anti-PPE57 (which recognizes a cell wall–associated protein control), and anti-Rv2145c (which recognizes a cytoplasmic protein) Abs.

Generation and culture of DCs

Bone marrow–derived cells from mice were collected and cultured as described previously (46). Over 82% of the nonadherent cells expressed CD11c after culturing them for 8 days in RPMI 1640 medium containing 10% FCS, 50 units/ml penicillin, 50 μg/ml streptomycin, IL-4 (500 IU/10^6 cells), and GM-CSF (1000 IU/10^6 cells) at 37 °C in a humidified incubator (5% CO_2). To obtain highly purified populations for the subsequent analyses, the DCs were labeled with bead-conjugated anti-CD11c (Miltenyi Biotec, Bergisch Gladbach, Germany) followed by positive selection with paramagnetic columns (LS columns, Miltenyi Biotec) according to the manufacturer's instructions. The purity of the DCs was ~92%.

Measurement of cytokine expression levels

DCs (1.0 $\times$ 10^6 cells/well) were cultured for 24 h with PBS alone, Pam3CSK4 (5 μg/ml), or PPE60 (1, 5, or 10 μg/ml). The production of IL-1β, TNFα, IL-8, IL-6, IL-10, IL-12 p70, and IL-23 p19 in the culture supernatants was determined by sandwich ELISA according to the manufacturer's instructions (BioLegend, San Diego, CA). For experiments designed to block TLR signaling, DCs (1.0 $\times$ 10^6 cells/well) were incubated for 1 h at 37 °C with a mouse isotype IgG (30 μg/ml) or with TLR2- or TLR4-specific Ab (30 μg/ml) (BioLegend).

Pharmacological inhibition of signaling pathways in DCs

All pharmacological inhibitors were obtained from Calbiochem. DCs (1.0 $\times$ 10^6 cells/well) were treated for 1 h with pharmacological inhibitors of p38 (SB203580; 20 μM), JNK (SP600125; 10 μM), and NF-κB (Bay11-7082; 20 μM) or with 0.1% (v/v) dimethyl sulfoxide (DMSO; Sigma) as a blank control followed by treatment with PPE60 (10 μg/ml) for 24 h.

Western blot analysis of kinase activation

DCs (1.0 $\times$ 10^6 cells/well) were treated with RPMI 1640 medium, PPE60 (10 μg/ml), Pam3CSK4 (5 μg/ml), or LPS (1 μg/ml) for 1 h at 37 °C and then lysed with cell lysis buffer (50 mM Tris-HCl, pH 7.5, 150 mM NaCl, 1% Triton^{TM} X-100, 1.0 mM EDTA, 50 mM NaF, 30 mM Na_4PO_7, 1.0 mM phenylmethanesulfonyl fluoride, 2.0 μg/ml aprotinin, 1.0 mM pervanadate) containing a protease inhibitor mixture (Roche Applied Science). To separate the cytoplasmic and nuclear fractions, the lysates were processed using the Cytoplasmic and NE-PER Nuclear Extraction kit (Pierce) according to the manufacturer's instructions (30). Western blotting was performed as described previously (28). Briefly, equal amounts of proteins were separated by SDS-PAGE on a 10% polyacrylamide gel and transferred electrophoretically to PVDF membranes (Millipore). Following treatment with 5% nonfat milk in Tris-buffered saline with Tween 20 (TBST) buffer, the membranes were incubated with the following primary Abs overnight at 4 °C: rabbit anti-ERK1/2, rabbit anti-p-ERK1/2, rabbit anti-p38, rabbit anti-p-p38, rabbit anti-JNK, rabbit anti-p-JNK, rabbit anti-NF-κB p65, rabbit anti-β-actin, or rabbit anti-GAPDH (Santa Cruz Biotechnology) according to the supplier's instructions. After washing with TBST buffer, membranes were incubated with an HRP-conjugated secondary Ab for 1–2 h at 37 °C. Target proteins were visualized using Pierce enhanced chemiluminescence (ECL) Western Blotting Substrate (Thermo Fisher Scientific).

Immunoprecipitation

DCs (5.0 $\times$ 10^6 cells/well) were treated with PPE60 (10 μg/ml) for 6 h at 37 °C followed by lysis with radioimmune

precipitation assay buffer (10 mM Tris-HCl, pH 7.4, 1% Nonidet P-40, 0.25% sodium deoxycholate, 150 mM NaCl, 1 mM EDTA, 1 mM PMSF, 1 μg/ml aprotinin, 1 μg/ml leupeptin, 1 μg/ml pepstatin, 1 mM Na_3VO_4, 1 mM NaF) (Sangon Biotech, Shanghai, China). The resulting lysates (1 mg) were incubated with 100 μl of 50% protein A- or G-Sepharose beads (Santa Cruz Biotechnology) for 2 h. Supernatants were incubated with isotype IgG (control), anti-TLR2, anti-TLR4, or anti-PPE60 Ab (Santa Cruz Biotechnology) overnight at 4 °C following centrifugation at 10,000 $\times$ *g* for 5 min at 4 °C. The beads were washed twice and boiled in 5$\times$ sample buffer for 5 min. Samples were electrophoresed on a 10% polyacrylamide gel with SDS, transferred to PVDF membranes (Millipore), and probed with anti-His, anti-TLR2, or anti-TLR4 Ab (Santa Cruz Biotechnology) followed by probing with the appropriate HRP-conjugated anti-IgG Ab. Target proteins were detected using an ECL reagent (Thermo Fisher Scientific).

Flow cytometry analysis of surface molecule expression and intracellular cytokine assays

DCs (1.0×10^6 cells/well) were treated for 24 h with PBS alone (control), various concentrations of PPE60 protein (1, 5, and 10 μg/ml), or 5 μg/ml Pam3CSK4. To evaluate the expression of surface molecules, cells were washed twice with prechilled PBS; centrifuged at 1000 $\times$ *g* for 10 min at 4 °C followed by treatment with Fc Block (BD Pharmingen) diluted in 1% BSA buffer; and then incubated with FITC-conjugated anti-mouse CD80, PE-conjugated anti-mouse CD86, or FITC-conjugated anti-mouse I-A/I-E Ab or with PE-conjugated anti-mouse H-2κB for mouse macrophages (BD Pharmingen) on ice for 30 min in the dark. In addition, to examine the intracellular expression of cytokines, DCs (1.0×10^6 cells/well) were incubated with FITC-conjugated CD11c Ab and the appropriate isotype-matched IgG (negative control) for 30 min at 4 °C. The cells were then fixed and permeabilized with a Cytofix/Cytoperm kit (BD Biosciences) following the manufacturer's instructions. The intracellular cytokines IL-12 p70 and IL-10 were labeled with PE-conjugated Abs (BD Pharmingen). The resulting data were analyzed using CellQuest data analysis and FlowJo 10.0 software (Tree Star, Inc., Ashland, OR).

Confocal microscopy analysis

DCs (1.0×10^6 cells/well) were seeded on coverslips and treated with RPMI 1640 medium or 10 μg/ml PPE60 for 1 h followed by fixation and permeabilization with cold methanol and 0.2% digitonin, respectively. After treatment with 2% BSA, cells were subjected to immunostaining with primary Abs specific to p-p38 and p-JNK for 4 h followed by Alexa Fluor 488 – or Alexa Fluor 555–conjugated secondary Ab for 2 h. Cells were then treated with 0.5 g/ml DAPI (Santa Cruz Biotechnology) for 5 min at 20 °C for visualization of nuclei. After washing with PBS twice, the slides were covered with coverslips using an antifade mountant kit (Thermo Fisher Scientific). Zeiss LSM 710 was used to observe target proteins using a 60$\times$ oil objective lens (Carl Zeiss, Oberkochen, Germany). Images were acquired using LSM 710 Meta software and analyzed using ImageJ (version 1.4.4).

Involvement of TLR in DC maturation induced by PPE60

DCs (1.0×10^6 cells/well) were treated with 30 μg/ml anti-TLR2, 30 μg/ml anti-TLR4, or 30 μg/ml isotype Ab (BD Pharmingen) followed by treatment with 0, 1, 5, 10, or 30 μg/ml PPE60 for 24 h. The quantities of IL-1β in the culture supernatant were determined by ELISA. DCs (1.0×10^6 cells/well) derived from WT and TLR2$^{-/-}$ mice were treated with PPE60 (10 μg/ml) for 1 h. After treatment with 5% BSA in PBS containing 5% goat serum and 0.1% Tween 20 for 2 h, cells were stained with a FITC-conjugated anti-His mAb. The cells were analyzed using a BD FACScan calibrator (BD Biosciences). In addition, DCs (1.0×10^6 cells/well) derived from WT, TLR2$^{-/-}$, and TLR4$^{-/-}$ mice were treated with PPE60 (10 μg/ml) for 1 h and then stained with DAPI (blue), anti-His Ab, or anti-TLR2 Ab. Cells were then observed using a 60$\times$ oil objective on a Zeiss LSM 710 confocal laser microscope. DCs (1×10^6 cells/well) from WT, TLR2$^{-/-}$, and TLR4$^{-/-}$ mice were stimulated for 24 h with 10 μg/ml PPE60, 100 ng/ml LPS, or 5 μg/ml Pam3CSK4. The cells were stained with PE-conjugated anti-mouse CD86 or FITC-conjugated anti-mouse I-A/I-E Ab for 30 min and then measured by flow cytometry. The levels of TNFα, IL-6, and IL-12 p70 in the supernatant were analyzed by ELISA.

Assessing MHC-II expression and antigen processing

The analysis of MHC-II expression and antigen processing was performed as described previously (57). DCs from C57BL/6 (5.0×10^5 cells/well) were treated for 24 or 48 h with medium, 15 ng/ml IFN-γ, 10–20 μg/ml PPE60, or 15 ng/ml IFN-γ + 10 μg/ml PPE60. Following treatment, cells were stained with anti-MHC-II or isotype IgG Abs for 30 min. MHC-II expression was determined using a flow cytometer. The resulting data were analyzed using CellQuest data analysis and FlowJo 10.0 software.

To determine the role of TLR2 in PPE60-enhanced MHC-II expression, DCs (5.0×10^5 cells/well) from C57BL/6 or TLR2$^{-/-}$ mice were treated for 24 or 48 h with medium, 15 ng/ml IFN-γ, 10 μg/ml PPE60, or 15 ng/ml IFN-γ + 10 μg/ml PPE60. MHC-II expression was detected as mentioned above. The Δ mean fluorescence value (ΔMFV) was defined as the MFV of cells labeled with MHC-II Abs minus the MFV of cells stained with isotype Abs.

For the CTLL-2 bioassay, DCs (5.0×10^5 cells/well) from C57BL/6, TLR2$^{-/-}$, or TLR4$^{-/-}$ mice were treated for 24 h with or without PPE60 at the indicated concentrations in the presence of 15 ng/ml IFN-γ (R&D Systems). Cells were then stimulated with the indicated concentration of OVA(323–339) for 3 h, fixed in 1% paraformaldehyde buffer, and cocultured with DOBW T-hybridoma cells (1.0×10^6 cells/well) for 24 h. Supernatants from the T-hybridoma assay were assessed for IL-2 using the CTLL-2 cell bioassay with Alamar Blue–based colorimetric determination (Alamar Biosciences, Sacramento, CA) and a Bio-Rad 550 microplate reader.

To examine the role of TLR2 in antigen processing, DCs were treated with Ab specific to isotype IgG, TLR2, or TLR4 for 18 h and then stimulated with or without 10 μg/ml PPE60 in the presence of IFN-γ (15 ng/ml) for 24 h. PPE60 Ag–specific

$CD4^+$ T cells were then cocultured with those DCs for 48 h at a ratio of 10:1 (T cells:DCs). Additionally, C57BL/6 mice or $TLR2^{-/-}$ mice (female, 6–8 weeks old, eight mice/group) were immunized subcutaneously three times over a 2-week period with 50 μg of PPE60 formulated with 250 μg of dimethyldioctadecylammonium (DDA) adjuvants (Sigma). DCs isolated from WT or $TLR2^{-/-}$ mice were then incubated with or without 10 μg/ml PPE60 in the presence of IFN-γ (15 ng/ml) for 24 h at 37 °C. DCs were then cocultured for 48 h with $CD4^+$ T cells isolated from PPE60-immunized mice at a ratio of 10:1 (T cells: DCs). IL-2 production was measured by ELISA following the manufacturer's instructions.

Analysis of the Th1/Th17 response

In the syngeneic mixed lymphocyte reaction, C57BL/6 mice (female, 6–8 weeks old, eight mice/group) were immunized subcutaneously three times over a 2-week period with 50 μg of Ag85B (ProSpec-Tany, Israel) formulated with DDA adjuvants. $CD4^+$ T cells were isolated from Ag85B-immunized mice, stained with carboxyfluorescein succinimidyl ester, and then cocultured for 72 h with DCs from mice that had been treated with PPE60 (10 μg/ml) or LPS (100 ng/ml) and then pulsed with Ag85B (10 μg/ml). T cells alone and T cells cocultured with untreated DCs served as controls. Cells were pulsed with 0.5 μCi [^{3}H]thymidine for 16 h. Cells were harvested in a Perkin-Elmer Life Sciences Filtermate harvester and counted in an LKB Rack Beta liquid scintillation counter (Model 1209, LKB-Wallac, Turku, Finland). Irradiated DCs alone incorporated between 40 and 90 cpm, whereas T cells alone incorporated between 280 and 970 cpm. IFN-γ, IL-2, IL-4, and IL-17A production in the supernatants of each sample was determined by ELISA. Cytokine production (IFN-γ, IL-4, and IL-17A) in $CD4^+$ T cells and the expression of GATA-3, T-bet, RORγt, and Foxp3 was measured using intracellular staining (BD Pharmingen).

To investigate the role of TLR2 in Th1/Th17 response induced by PPE60, C57BL/6 mice (female, 6–8 weeks old, eight mice/group) were immunized subcutaneously three times over a 2-week period with 50 μg of PPE60 formulated with 250 μg of DDA adjuvants. Responder T cells were isolated from splenocytes of PPE60-immunized C57BL/6 mice using CD4 magnetic beads (BD Biosciences). DCs (5.0×10^5 cells/well) were isolated from C57BL/6 or $TLR2^{-/-}$ mice as described above and treated with PBS, PPE60 (10 μg/ml), or Pam3CSK4 (5 μg/ml) for 24 h. T cells and DCs were then cocultured at a ratio of 10:1 for 3 days at 37 °C. T cells alone and T cells cocultured with untreated DCs served as controls. Sandwich ELISA kits were used to detect the levels of IFN-γ, IL-2, IL-4, and IL-17A in the resulting culture supernatants according to the manufacturer's instructions (BioLegend). The expression of GATA-3, T-bet, and RORγt was measured using Western blotting.

NLRP3, active caspase-1, and IL-1β assays

DCs were stimulated for 18 h with 10 μg/ml PPE60 or 5 μg/ml recombinant ESAT-6 protein expressed as described previously (53), stained for intracellular NLRP3 and active casp-1, and analyzed using confocal microscopy. In addition, cells prepared from DCs following stimulation with purified ESAT-6 or PPE60 were analyzed by Western blotting using anti-NLRP3, anti-NLRP1 (sc-390133, Santa Cruz Biotechnology), anti-casp-1, anti-IL-18, or anti-ASC Ab. DCs (1.0×10^6 cells/well) treated for 18 h with PPE60 or ESAT-6 (10 μg/ml) were stained for intracellular casp-1, NLRP3, IL-1β, and IL-18 using specifically labeled mAbs followed by staining with FITC-conjugated IgG, PE-conjugated IgG, or PE-Cy7–conjugated IgG (BD Pharmingen), respectively. Samples were processed for flow cytometry. For each sample, 10,000 events were recorded. Data were analyzed using BD FACSDIVA software (BD Biosciences). For the pharmacological inhibition assay, DCs from C57BL/6 mice were stimulated for 18 h with PBS, 10 μg/ml PPE60, or 5 μg/ml ESAT-6 (ProSpec-Tany, Israel) in the presence or absence of 10 mmol/ml MCC950 (CP-456773). The levels of IL-1β and IL-18 were measured by ELISA kits.

To determine whether inflammasome activation by PPE60 is TLR2-dependent, DCs (1.0×10^6 cells/well) isolated from C57BL/6 or $TLR2^{-/-}$ mice were treated for 18 h with PPE60 or ESAT-6 (10 μg/ml) and analyzed by Western blotting using anti-NLRP3, anti-casp-1, anti-IL-18, or anti-ASC Ab. The levels of IL-1β and IL-18 were measured by ELISA kits.

For the pharmacological inhibition assay, naïve T cells from PPE60-immunized or ESAT-6–immunized C57BL/6 mice (female, 6–8 weeks old) were prepared using MACS columns (Miltenyi Biotec) according to the manufacturer's instructions. The purity of naïve T cells was >95% as measured by flow cytometry. DCs from C57BL/6 mice were stimulated for 18 h with medium, 10 μg/ml PPE60, or 5 μg/ml ESAT-6; simultaneously incubated with 10 mmol/ml MCC950 (CP-456773) or 5 mmol/ml Z-YVAD-fmk (S810202) in the presence or absence of 50 units/ml rhIL-1β for 18 h; and then cocultured with $CD4^+$ T cells (1×10^6 cells/well) for 48 h at a 1:10 ratio, respectively. T-cell response was determined by measuring IFN-γ and IL-17 production in the supernatant by ELISA.

Statistical analysis

To determine the statistical significance of the data, results were analyzed using Student's *t* test for simple comparison or one-way analysis of variance with Tukey's correction for multiple comparisons using Origin 8.0 software (Origin Lab, Northampton, MA).

Author contributions—H. S. and Y. X. resources; H. S., Zhen Zhang, Z. L., B. P., C. K., and Y. X. data curation; H. S., Zhen Zhang, Z. L., and Y. X. software; H. S. and Y. X. formal analysis; H. S., C. K., H. W., and Y. X. validation; H. S. and Y. X. investigation; H. S., Zhi Zhang, and Y. X. visualization; H. S., Zhen Zhang, and Y. X. methodology; H. S. and Y. X. writing-original draft; H. S. and Y. X. writing-review and editing; C. K. and Y. X. funding acquisition; Zhi Zhang and Y. X. project administration; Y. X. conceptualization; Y. X. supervision.

References

1. Nieuwenhuizen, N. E., and Kaufmann, S. H. E. (2018) Next-generation vaccines based on Bacille Calmette-Guerin. *Front. Immunol.* **9,** 121 CrossRef Medline
2. O'Garra, A., Redford, P. S., McNab, F. W., Bloom, C. I., Wilkinson, R. J., and Berry, M. P. (2013) The immune response in tuberculosis. *Annu. Rev. Immunol.* **31,** 475–527 CrossRef Medline

3. Sayes, F., Sun, L., Di Luca, M., Simeone, R., Degaiffier, N., Fiette, L., Esin, S., Brosch, R., Bottai, D., Leclerc, C., and Majlessi, L. (2012) Strong immunogenicity and cross-reactivity of *Mycobacterium tuberculosis* ESX-5 type VII secretion: encoded PE-PPE proteins predicts vaccine potential. *Cell Host Microbe* **11,** 352–363 CrossRef Medline
4. Kaufmann, S. H., and Gengenbacher, M. (2012) Recombinant live vaccine candidates against tuberculosis. *Curr. Opin. Biotechnol.* **23,** 900–907 CrossRef Medline
5. Andersen, P., and Doherty, T. M. (2005) The success and failure of BCG—implications for a novel tuberculosis vaccine. *Nat. Rev.. Microbiol.* **3,** 656–662 CrossRef Medline
6. Brennan, M. J. (2017) The enigmatic PE/PPE multigene family of mycobacteria and tuberculosis vaccination. *Infect. Immun.* **85,** e00969-16 CrossRef Medline
7. Fishbein, S., van Wyk, N., Warren, R. M., and Sampson, S. L. (2015) Phylogeny to function: PE/PPE protein evolution and impact on *Mycobacterium tuberculosis* pathogenicity. *Mol. Microbiol.* **96,** 901–916 CrossRef Medline
8. Vordermeier, H. M., Hewinson, R. G., Wilkinson, R. J., Wilkinson, K. A., Gideon, H. P., Young, D. B., and Sampson, S. L. (2012) Conserved immune recognition hierarchy of mycobacterial PE/PPE proteins during infection in natural hosts. *PLoS One* **7,** e40890 CrossRef Medline
9. Camacho, L. R., Ensergueix, D., Perez, E., Gicquel, B., and Guilhot, C. (1999) Identification of a virulence gene cluster of *Mycobacterium tuberculosis* by signature-tagged transposon mutagenesis. *Mol. Microbiol.* **34,** 257–267 CrossRef Medline
10. Sassetti, C. M., and Rubin, E. J. (2003) Genetic requirements for mycobacterial survival during infection. *Proc. Natl. Acad. Sci. U.S.A.* **100,** 12989–12994 CrossRef Medline
11. Li, Y., Miltner, E., Wu, M., Petrofsky, M., and Bermudez, L. E. (2005) A *Mycobacterium avium* PPE gene is associated with the ability of the bacterium to grow in macrophages and virulence in mice. *Cell. Microbiol.* **7,** 539–548 CrossRef Medline
12. Mukhopadhyay, S., and Balaji, K. N. (2011) The PE and PPE proteins of *Mycobacterium tuberculosis*. *Tuberculosis* **91,** 441–447 CrossRef Medline
13. Sampson, S. L. (2011) Mycobacterial PE/PPE proteins at the host-pathogen interface. *Clin. Dev. Immunol.* **2011,** 497203 CrossRef Medline
14. Comas, I., Chakravartti, J., Small, P. M., Galagan, J., Niemann, S., Kremer, K., Ernst, J. D., and Gagneux, S. (2010) Human T cell epitopes of *Mycobacterium tuberculosis* are evolutionarily hyperconserved. *Nat. Genet.* **42,** 498–503 CrossRef Medline
15. Brennan, M. J., and Delogu, G. (2002) The PE multigene family: a 'molecular mantra' for mycobacteria. *Trends Microbiol.* **10,** 246–249 CrossRef Medline
16. Voskuil, M. I., Schnappinger, D., Rutherford, R., Liu, Y., and Schoolnik, G. K. (2004) Regulation of the *Mycobacterium tuberculosis* PE/PPE genes. *Tuberculosis* **84,** 256–262 CrossRef Medline
17. Akhter, Y., Ehebauer, M. T., Mukhopadhyay, S., and Hasnain, S. E. (2012) The PE/PPE multigene family codes for virulence factors and is a possible source of mycobacterial antigenic variation: perhaps more? *Biochimie* **94,** 110–116 CrossRef Medline
18. Sato, K., Akaki, T., and Tomioka, H. (1998) Differential potentiation of anti-mycobacterial activity and reactive nitrogen intermediate-producing ability of murine peritoneal macrophages activated by interferon-γ (IFN-γ) and tumour necrosis factor-α (TNF-α). *Clin. Exp. Immunol.* **112,** 63–68 CrossRef Medline
19. Gopal, R., Monin, L., Slight, S., Uche, U., Blanchard, E., Fallert Junecko, B. A., Ramos-Payan, R., Stallings, C. L., Reinhart, T. A., Kolls, J. K., Kaushal, D., Nagarajan, U., Rangel-Moreno, J., and Khader, S. A. (2014) Unexpected role for IL-17 in protective immunity against hypervirulent *Mycobacterium tuberculosis* HN878 infection. *PLoS Pathog.* **10,** e1004099 CrossRef Medline
20. García Jacobo, R. E., Serrano, C. J., Enciso Moreno, J. A., Gaspar Ramírez, O., Trujillo Ochoa, J. L., Uresti Rivera, E. E., Portales Pérez, D. P., González-Amaro, R., and García Hernández, M. H. (2014) Analysis of Th1, Th17 and regulatory T cells in tuberculosis case contacts. *Cell. Immunol.* **289,** 167–173 CrossRef Medline
21. Jang, S., Uzelac, A., and Salgame, P. (2008) Distinct chemokine and cytokine gene expression pattern of murine dendritic cells and macrophages in response to *Mycobacterium tuberculosis* infection. *J. Leukoc. Biol.* **84,** 1264–1270 CrossRef Medline
22. de Souza, G. A., Leversen, N. A., Målen, H., and Wiker, H. G. (2011) Bacterial proteins with cleaved or uncleaved signal peptides of the general secretory pathway. *J. Proteomics* **75,** 502–510 CrossRef Medline
23. Bertholet, S., Ireton, G. C., Kahn, M., Guderian, J., Mohamath, R., Stride, N., Laughlin, E. M., Baldwin, S. L., Vedvick, T. S., Coler, R. N., and Reed, S. G. (2008) Identification of human T cell antigens for the development of vaccines against *Mycobacterium tuberculosis*. *J. Immunol.* **181,** 7948–7957 CrossRef Medline
24. Kruh, N. A., Troudt, J., Izzo, A., Prenni, J., and Dobos, K. M. (2010) Portrait of a pathogen: The Mycobacterium tuberculosis proteome *in vivo*. PLoS One **5,** e13938 Medline CrossRef
25. Derrick, S. C., Yabe, I. M., Yang, A., Kolibab, K., Hollingsworth, B., Kurtz, S. L., and Morris, S. (2013) Immunogenicity and protective efficacy of novel *Mycobacterium tuberculosis* antigens. *Vaccine* **31,** 4641–4646 CrossRef Medline
26. Windish, H. P., Duthie, M. S., Misquith, A., Ireton, G., Lucas, E., Laurance, J. D., Bailor, R. H., Coler, R. N., and Reed, S. G. (2011) Protection of mice from *Mycobacterium tuberculosis* by ID87/GLA-SE, a novel tuberculosis subunit vaccine candidate. *Vaccine* **29,** 7842–7848 CrossRef Medline
27. Sayes, F., Pawlik, A., Frigui, W., Gröschel, M. I., Crommelynck, S., Fayolle, C., Cia, F., Bancroft, G. J., Bottai, D., Leclerc, C., Brosch, R., and Majlessi, L. (2016) CD4+ T cells recognizing PE/PPE antigens directly or via cross reactivity are protective against pulmonary *Mycobacterium tuberculosis* infection. *PLoS Pathog.* **12,** e1005770 CrossRef Medline
28. Xu, Y., Yang, E., Huang, Q., Ni, W., Kong, C., Liu, G., Li, G., Su, H., and Wang, H. (2015) PPE57 induces activation of macrophages and drives Th1-type immune responses through TLR2. *J. Mol. Med.* **93,** 645–662 CrossRef Medline
29. Thakker, P., Leach, M. W., Kuang, W., Benoit, S. E., Leonard, J. P., and Marusic, S. (2007) IL-23 is critical in the induction but not in the effector phase of experimental autoimmune encephalomyelitis. *J. Immunol.* **178,** 2589–2598 CrossRef Medline
30. Su, H., Kong, C., Zhu, L., Huang, Q., Luo, L., Wang, H., and Xu, Y. (2015) PPE26 induces TLR2-dependent activation of macrophages and drives Th1-type T-cell immunity by triggering the cross-talk of multiple pathways involved in the host response. *Oncotarget* **6,** 38517–38537 CrossRef Medline
31. Nair, S., Ramaswamy, P. A., Ghosh, S., Joshi, D. C., Pathak, N., Siddiqui, I., Sharma, P., Hasnain, S. E., Mande, S. C., and Mukhopadhyay, S. (2009) The PPE18 of *Mycobacterium tuberculosis* interacts with TLR2 and activates IL-10 induction in macrophage. *J. Immunol.* **183,** 6269–6281 CrossRef Medline
32. Ade, N., Antonios, D., Kerdine-Romer, S., Boisleve, F., Rousset, F., and Pallardy, M. (2007) NF-κB plays a major role in the maturation of human dendritic cells induced by $NiSO_4$ but not by DNCB. *Toxicol. Sci.* **99,** 488–501 CrossRef Medline
33. Lewinsohn, D. A., Lewinsohn, D. M., and Scriba, T. J. (2017) Polyfunctional $CD4^+$ T cells as targets for tuberculosis vaccination. *Front. Immunol.* **8,** 1262 CrossRef Medline
34. Briken, V., Ahlbrand, S. E., and Shah, S. (2013) *Mycobacterium tuberculosis* and the host cell inflammasome: a complex relationship. *Front. Cell. Infect. Microbiol.* **3,** 62 CrossRef Medline
35. Dorhoi, A., Nouailles, G., Jörg, S., Hagens, K., Heinemann, E., Pradl, L., Oberbeck-Müller, D., Duque-Correa, M. A., Reece, S. T., Ruland, J., Brosch, R., Tschopp, J., Gross, O., and Kaufmann, S. H. (2012) Activation of the NLRP3 inflammasome by *Mycobacterium tuberculosis* is uncoupled from susceptibility to active tuberculosis. *Eur. J. Immunol.* **42,** 374–384 CrossRef Medline
36. Kupz, A., Zedler, U., Stäber, M., Perdomo, C., Dorhoi, A., Brosch, R., and Kaufmann, S. H. (2016) ESAT-6-dependent cytosolic pattern recognition drives noncognate tuberculosis control *in vivo*. *J. Clin. Investig.* **126,** 2109–2122 CrossRef Medline
37. Fernandes-Alnemri, T., Kang, S., Anderson, C., Sagara, J., Fitzgerald, K. A., and Alnemri, E. S. (2013) Cutting edge: TLR signaling licenses IRAK1

for rapid activation of the NLRP3 inflammasome. *J. Immunol.* **191,** 3995–3999 CrossRef Medline

38. Sia, J. K., Georgieva, M., and Rengarajan, J. (2015) Innate immune defenses in human tuberculosis: an overview of the interactions between *Mycobacterium tuberculosis* and innate immune Cells. *J. Immunol. Res.* **2015,** 747543 CrossRef Medline
39. Yuk, J. M., and Jo, E. K. (2014) Host immune responses to mycobacterial antigens and their implications for the development of a vaccine to control tuberculosis. *Clin. Exp. Vaccine Res.* **3,** 155–167 CrossRef Medline
40. Basu, S., Pathak, S. K., Banerjee, A., Pathak, S., Bhattacharyya, A., Yang, Z., Talarico, S., Kundu, M., and Basu, J. (2007) Execution of macrophage apoptosis by PE_PGRS33 of *Mycobacterium tuberculosis* is mediated by Toll-like receptor 2-dependent release of tumor necrosis factor-alpha. *J. Biol. Chem.* **282,** 1039–1050 CrossRef Medline
41. Bansal, K., Sinha, A. Y., Ghorpade, D. S., Togarsimalemath, S. K., Patil, S. A., Kaveri, S. V., Balaji, K. N., and Bayry, J. (2010) Src homology 3-interacting domain of Rv1917c of *Mycobacterium tuberculosis* induces selective maturation of human dendritic cells by regulating PI3K-MAPK-NF-κB signaling and drives Th2 immune responses. *J. Biol. Chem.* **285,** 36511–36522 CrossRef Medline
42. Bansal, K., Elluru, S. R., Narayana, Y., Chaturvedi, R., Patil, S. A., Kaveri, S. V., Bayry, J., and Balaji, K. N. (2010) PE_PGRS antigens of *Mycobacterium tuberculosis* induce maturation and activation of human dendritic cells. *J. Immunol.* **184,** 3495–3504
43. Gopalakrishnan, A., and Salgame, P. (2016) Toll-like receptor 2 in host defense against *Mycobacterium tuberculosis*: to be or not to be-that is the question. *Curr. Opin. Immunol.* **42,** 76–82 CrossRef Medline
44. Forsyth, K. S., and Eisenlohr, L. C. (2016) Giving CD4+ T cells the slip: viral interference with MHC class II-restricted antigen processing and presentation. *Curr. Opin. Immunol.* **40,** 123–129 CrossRef Medline
45. Saini, N. K., Baena, A., Ng, T. W., Venkataswamy, M. M., Kennedy, S. C., Kunnath-Velayudhan, S., Carreño, L. J., Xu, J., Chan, J., Larsen, M. H., Jacobs, W. R., Jr., and Porcelli, S. A. (2016) Suppression of autophagy and antigen presentation by *Mycobacterium tuberculosis* PE_PGRS47. *Nat. Microbiol.* **1,** 16133 CrossRef Medline
46. Kim, W. S., Kim, J. S., Cha, S. B., Kim, S. J., Kim, H., Kwon, K. W., Han, S. J., Choi, S. Y., and Shin, S. J. (2016) Mycobacterium tuberculosis PE27 activates dendritic cells and contributes to Th1-polarized memory immune responses during *in vivo* infection. *Immunobiology* **221,** 440–453 CrossRef Medline
47. Mourik, B. C., Lubberts, E., de Steenwinkel, J. E. M., Ottenhoff, T. H. M., and Leenen, P. J. M. (2017) Interactions between type 1 interferons and the Th17 response in tuberculosis: lessons learned from autoimmune diseases. *Front. Immunol.* **8,** 294 CrossRef Medline
48. Khubaib, M., Sheikh, J. A., Pandey, S., Srikanth, B., Bhuwan, M., Khan, N., Hasnain, S. E., and Ehtesham, N. Z. (2016) *Mycobacterium tuberculosis* co-operonic PE32/PPE65 proteins alter host immune responses by hampering Th1 response. *Front. Microbiol.* **7,** 719 CrossRef Medline
49. Baldwin, S. L., Bertholet, S., Kahn, M., Zharkikh, I., Ireton, G. C., Vedvick, T. S., Reed, S. G., and Coler, R. N. (2009) Intradermal immunization improves protective efficacy of a novel TB vaccine candidate. *Vaccine* **27,** 3063–3071 CrossRef Medline
50. Cruz, A., Fraga, A. G., Fountain, J. J., Rangel-Moreno, J., Torrado, E., Saraiva, M., Pereira, D. R., Randall, T. D., Pedrosa, J., Cooper, A. M., and Castro, A. G. (2010) Pathological role of interleukin 17 in mice subjected to repeated BCG vaccination after infection with *Mycobacterium tuberculosis*. *J. Exp. Med.* **207,** 1609–1616 CrossRef Medline
51. Chen, X., Zhou, B., Li, M., Deng, Q., Wu, X., Le, X., Wu, C., Larmonier, N., Zhang, W., Zhang, H., Wang, H., and Katsanis, E. (2007) $CD4^+CD25^+FoxP3^+$ regulatory T cells suppress *Mycobacterium tuberculosis* immunity in patients with active disease. *Clin. Immunol.* **123,** 50–59 CrossRef Medline
52. Mariathasan, S., and Monack, D. M. (2007) Inflammasome adaptors and sensors: intracellular regulators of infection and inflammation. *Nat. Rev. Immunol.* **7,** 31–40 CrossRef Medline
53. Mishra, B. B., Moura-Alves, P., Sonawane, A., Hacohen, N., Griffiths, G., Moita, L. F., and Anes, E. (2010) *Mycobacterium tuberculosis* protein ESAT-6 is a potent activator of the NLRP3/ASC inflammasome. *Cell. Microbiol.* **12,** 1046–1063 CrossRef Medline
54. Basu, S., Fowler, B. J., Kerur, N., Arnvig, K. B., and Rao, N. A. (2018) NLRP3 inflammasome activation by mycobacterial ESAT-6 and dsRNA in intraocular tuberculosis. *Microb. Pathog.* **114,** 219–224 CrossRef Medline
55. Donà, V., Ventura, M., Sali, M., Cascioferro, A., Provvedi, R., Palù, G., Delogu, G., and Manganelli, R. (2013) The PPE domain of PPE17 is responsible for its surface localization and can be used to express heterologous proteins on the mycobacterial surface. *PLoS One* **8,** e57517 CrossRef Medline
56. Cascioferro, A., Daleke, M. H., Ventura, M., Donà, V., Delogu, G., Palù, G., Bitter, W., and Manganelli, R. (2011) Functional dissection of the PE domain responsible for translocation of PE_PGRS33 across the mycobacterial cell wall. *PLoS One* **6,** e27713 CrossRef Medline
57. Noss, E. H., Pai, R. K., Sellati, T. J., Radolf, J. D., Belisle, J., Golenbock, D. T., Boom, W. H., and Harding, C. V. (2001) Toll-like receptor 2-dependent inhibition of macrophage class II MHC expression and antigen processing by 19-kDa lipoprotein of *Mycobacterium tuberculosis*. *J. Immunol.* **167,** 910–918 CrossRef Medline